“ENERGY EXERGY ANALYSIS OF SOLAR CHIMNEY DRYING SYSTEM”

A DISSERTATION

SUBMITTED IN PARTIAL FULFILMENT OF THE REQUIREMENTS FOR THE AWARD OF THE DEGREE OF

MASTER OF TECHNOLOGY

IN

THERMAL ENGINEERING

Submitted by

SUDHANSHU DUTTA

(Roll No. 2K17/THE/16)

Under the supervision of

PROF. SAMSHER

&

DR. ANIL KUMAR

DEPARTMENT OF MECHANICAL ENGINEERING

DELHI TECHNOLOGICAL UNIVERSITY

(Formerly Delhi College of Engineering)

Bawana Road, Delhi-110042

OCTOBER, 2019

DELHI TECHNOLOGICAL UNIVERSITY

(Formerly Delhi College of Engineering)

Bawana Road, Delhi-110042

CANDIDATE'S DECLARATION

I, SUDHANSHU DUTTA, Roll No. 2K17/THE/16 student of M.Tech (Thermal Engineering), hereby declare that the project Dissertation titled "ENERGY EXERGY ANALYSIS OF SOLAR CHIMNEY DRYING SYSTEM" which is submitted by me to the Department of Mechanical Engineering, Delhi Technological University, Delhi in partial fulfillment of the requirement for the award of the degree of Master of Technology, is original and not copied from any source without proper citation. This work has not previously formed the basis for the award of any degree, Diploma Associateship, Fellowship or other similar title or recognition.

Place: Delhi **SUDHANSHU DUTTA**

Date:

DEPARTMENT OF MECHANICAL ENGINEERING

DELHI TECHNOLOGICAL UNIVERSITY

(Formerly Delhi College of Engineering)

Bawana Road, Delhi-110042

CERTIFICATE

It is certified that the Project Dissertation titled "ENERGY EXERGY ANALYSIS OF SOLAR CHIMNEY DRYING SYSTEM" which is being submitted by SUDHANSHU DUTTA, Roll No. 2k17/THE/16, Department of Mechanical Engineering, Delhi Technological University, Delhi in partial fulfillment of the requirement for the award of the degree of Master of Technology, is a record of the project work carried by the student under our supervision. To the best of our knowledge this work has not been submitted in part or full for any Degree of Diploma to this University or elsewhere.

(**DR. ANIL KUMAR**)	(**PROF. SAMSHER)**
SUPERVISOR	**SUPERVISOR**
ASSOCIATE PROFESSOR	**PROFESSOR**

Place: Delhi

Date

ACKNOWLEDGEMENT

Any accomplishment is a result of positivity of thoughts and efforts. It is important here to appreciate contribution, encouragement and support from person who stood as 'Light House' throughout the voyage.

I take great pride in expressing my unfeigned appreciation and gratitude to my learned mentors Prof. Samsher and Dr. Anil Kumar, Department of Mechanical Engineering, Delhi Technological University, Delhi for their invaluable inspiration, guidance and continuous encouragement throughout this project work. Working under their guidance has been a privilege and an excellent learning experience that I will cherish for a long time.

I also appreciate and acknowledge the efforts of all those who have, directly or indirectly, helped me achieving my aim.

SUDHANSHU DUTTA

(Roll No. 2k17/THE/16)

M.Tech (Thermal Engineering)

Delhi Technological University, Delhi, India

ABSTRACT

Experimental setup was situated on the rooftop of the Delhi Technological University (DTU), Delhi, India (28.75^0 N, 77.11^0 E). SCPP converts solar energy into electricity. In this thesis work, the effect of convective heat transfer coefficient, heat loss factor, heat utilization factor, diffusivity coefficient and instantaneous thermal loss efficiency factor, the design and experimental analysis of system with traditional cylindrical SCPP with solar dryer under the condition of natural convection in passive mode was carried out on hourly basis from 08:00 hours to 18:00 hours. The approach of exergy analysis is also investigating the thermodynamic understanding of the SCPP. Day 1 and day 2 were clear sky, while day 3 was cloudy. And the tests were carried out only in barren conditions of the ground. The convective heat transfer coefficient ranges from 1.29 $W/m^2\ ^0C$ to 2.60 $W/m^2\ ^0C$. The HUF ranges from 0.08 – 0.57 and COP ranges from 0.42 – 0.91. The exergetic efficiency of drying system under passive mode ranges from 23.49% – 92.74%. Heat loss factor value varies from 3.93 watts – 51.93 watts and the variation of coefficient of diffusivity value is from 0.003130 to 0.003172. The characteristic equation has been used for experimental results of solar drying system under passive mode to generate linear characteristic equation for clear sky condition. The instantaneous indirect loss efficiency curve have also been analyzed which shows the degree of effectiveness of the system. Also the experimental uncertainty analysis for ambient and ground temperature is calculated as 0.38% and 0.40% respectively which comes out to be within the permissible limit. The maximum temperature attained was 64.2^0C hence solar dryer can be recommended for drying corn, maize, paddy, pulses, tice, wheat, brinjal, cabbage, garlic, onion, tomatoes.

TABLE OF CONTENTS

LIST OF FIGURES

LIST OF TABLES

NOMENCLATURE

h_{cv}	Convective heat transfer coefficient of air (W/m^2 ^{0}C).
h_r	Radiative heat transfer coefficient (W/m^2 ^{0}C).
T_{gd}	Ground temperature (^{0}C).
T_{amb}	Ambient temperature (^{0}C).
$T_{ch,in}$	Chimney inlet temperature (^{0}C).
$T_{ch,out}$	Chimney outlet temperature (^{0}C).
$P(T)$	Vapor Pressure of humid air at temperature T (N/m^2).
Rh_{amb}	Ambient Relative humidity (%).
Rh_{in}	Relative humidity inside canopy (%).
V_{canopy}	Velocity at entry point of canopy (m/sec).
υ	Velocity on outer surface of canopy (m/sec).
σ	Stefan–Boltzmann constant (W/m^2 K^4).
U	Overall heat transfer coefficient (W/m^2 ^{0}C).
$\eta ith, canopy$	Instantaneous indirect thermal loss efficiency of canopy.
A_i	Surface area of canopy or greenhouse (m^2).
I_g	Global solar radiation (W/m^2).
I_d	Diffused solar radiation (W/m^2).
A_{tray}	Effective area of drying tray (m^2).
$\eta ith, vent$	Instantaneous indirect thermal loss efficiency of vent.
C_{df}	Coefficient of diffusivity.
$A_{chimney}$	Area of chimney (m^2).
ΔP	Partial pressure difference between greenhouse temperature air And ambient air (N/m^2).
ρ	Density of greenhouse air (kg/m^3)
n	No. of vents.
Q_{lf}	Heat loss factor (watts).

HUF	Heat utilization factor.
COP	Coefficient of performance.
$m_{amb.}$	Mass flow rate of ambient air entering the greenhouse (kg/sec)
$C_{p,dry\ amb}$	Specific heat at constant pressure of air used for drying inside Greenhouse (KJ/Kg ^{0}C).
$E_{x\ loss}$	Exergy losses during the passive mode of drying process.
$E_{x\ inlet}$	Exergy where air is entering the greenhouse (KW).
$E_{x\ outlet}$	Exergy where air is exiting the greenhouse (KW).
$E_{x\ loss}$	Exergy losses during the passive mode of drying process (KW).
η_{Ex}	Exergetic efficiency of the system.
U'	Internal uncertainty.
σ'	Standard deviation.
N	Number of sets.
N_0'	Number of observation in each set.
$(X_i - \bar{X})$	Deviation from mean.
l_g	Thickness of PVC sheet (meters).
K	Thermal conductivity of PVC sheet (W/m ^{0}C).

ABBREVIATION

PV	Photovoltaic
IEA	International Energy Agency
INDC	Intended Nationally Determined Contributions
CAGR	Compound Annual Growth Rate
MNRE	Ministry of New and Renewable Energy
COP-21	Conference of the Parties 21
UNFCCC	United Nations Framework Convention on Climate Change
GHG	Greenhouse Gases
GDP	Gross Domestic Products
NSM	National Solar Mission
NAPCC	National Action Plan on Climate Change
SCPP	Solar Chimney Power Plant
PVC	Polyvinyl Chloride
DSPP	Divergent chimney solar power plants
COAR	Chimney outlet to inlet area ratio
PCM	Phase change materials
BLS	Boundary layer separation
SUT	Solar updraft tower
DO	Discrete ordinates
GRFP	Glass fiber reinforced plastics
CFD	Computational fluid dynamic
MGD	Modified greenhouse dryer
AM	Active Mode
PM	Passive Mode
CO_2	Carbon dioxide

CHAPTER-1

INTRODUCTION

1.1 WORLD'S ENERGY SCENARIO

World's energy demand is increasing remarkably as global population is growing at a significant rate and to meet this huge demand of energy, generation of energy at notably higher rate is required. In 21st century, energy demand-supply is taken as one of the most casual issue. Different countries have different strategies and plans to overcome this energy crisis [1] . Due to surplus use of conventional fossil fuels to meet energy demand, the environment is declining and worsening. Ecosystem is polluted because of harmful emissions on burning of fossil fuels, mining, deforestation etc. [2]. World's 80% energy is generated by the use of conventional sources so there is need of urgency to shift the energy production towards renewable sources. Amongst non-conventional sources, solar energy is be the best alternative because firstly, it has plentiful energy capacity among all the renewable sources of energy. The sun emits 3.8×10^{23} Kilowatts of energy out of which only 1.8×10^{14} Kilowatts is trapped by the earth [3]. Secondly, it is free of cost and present in abundance [4]. Thirdly, it provides increasing efficiency when compared among all renewable sources. Solar radiation and intensity of the radiation are two important factors that concludes the efficiency of solar PV industry [5]. Since 2010, the global primary energy rose by 2.9% in 2018 which is the maximum growth. Worldwide approximately 520 quadrillion Btu has been consumed till 2011 [6].The sudden and rapid growth of the energy was met together by renewable and nuclear energy. Nevertheless, generation from conventional power plants have increased significantly to cope up with the higher demand for electricity, increasing the sector's CO_2 emissions by 2.5%. Emissions from power generation last year exceeded nearly 13 Gt, or 38% of total CO_2 emissions.

Growth in renewable generation has accelerated from 6% in 2017 to 7% in 2018 and has reached 45% of global demand for electricity. Fig 1.2 shows that solar photovoltaic accounts for 30% while both, hydropower and wind power accounts for 29% of global renewable energy production. Amongst rest of the sources of energy, bioenergy has the maximum share. The generation of nuclear power increased by 3.3% and the reason for

half of this was due to the commissioning of new plants in China. In 2018, conventional power plants were also called on to cope up with the increasing demand for electricity, given the significant increase in production from low-carbon sources. Coal rose in 2018 more than any other single generation origin, representing 26% of the total additional generation. It remains the largest source of electricity generation with a market share of 38 percent.

China along with the U.S.A, accounted for 70 percent of global increase in demand. In China, compared to recent years, there has been a large increase in demand for electricity by 8.5 percent and it was driven by combination of industries of coal, steel materials, cement, and increased cooling demand. Fig 1.1 shows that growth in renewable electricity generation in 2018 is maximum for china followed by Europe In the United States, after stable consumption in recent years, demand jumped by record level of almost 4000 TWh, 17% of the global total. The major reason of record level increasing demand was because the region experienced the hottest summer and the coldest winters [7]. Due to higher electricity demand, global CO_2 emissions increased by up to 1.7%. As fossil-fuel-based energy increased, power sector accounted for two-thirds of emission rise, mostly in Asia. About 85 percent gross increase in CO_2 emissions was accounted India, China & U.S.A, while significant CO_2 emissions decreasing trend was seen for Japan, Germany, France, Mexico, & the UK. Fig 1.3 depicts that even though, during 2014-2016, the world's economy kept on growing but CO_2 emissions growth rate became constant. The reason behind was deployment of energy efficient and low carbon technology which lead to depreciation of coal demand. But in the years 2017 and 2018, the situation changed as increasing energy production failed to cope up with economic growth and also low carbon technology could not level up to cope up with this demand.

IEA measured the impact of using fossil fuels on the increase in global temperature for the first time. The effect of coal combustion energy production accounted for 0.3^0 C out of 1^0 C rise in pre-industrial pre industrial annual global surface temperature. It thus makes carbon the largest single cause of the annual average increase in global temperature.

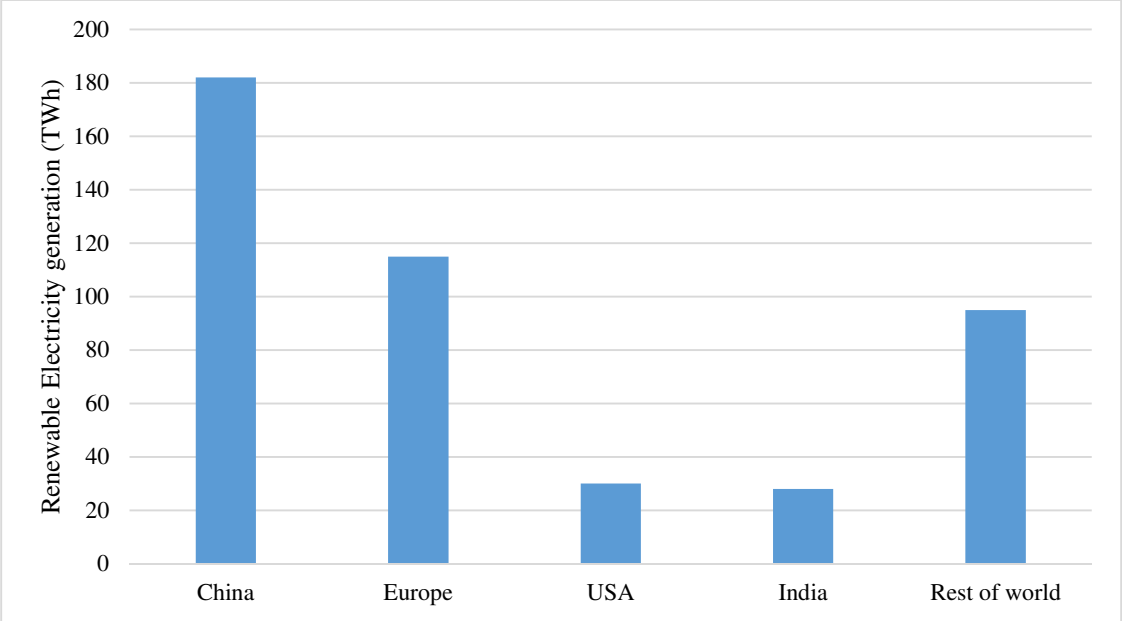

Fig 1.1: Global growth in Renewable electricity generation by region, 2018 [7].

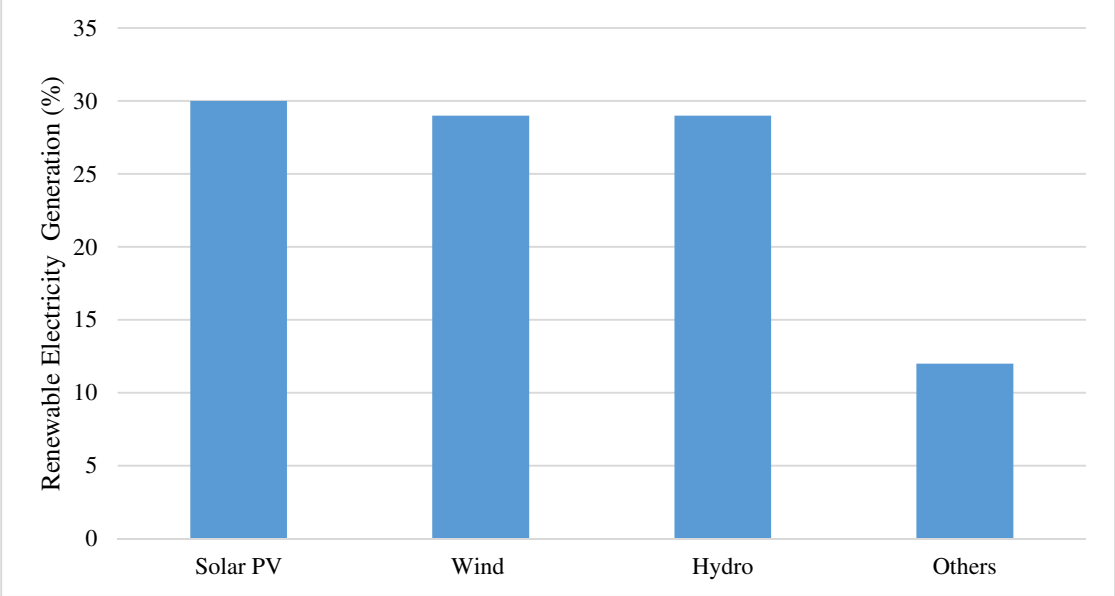

Fig 1.2: Percent growth in renewable electricity generation by different technology, 2018 [7].

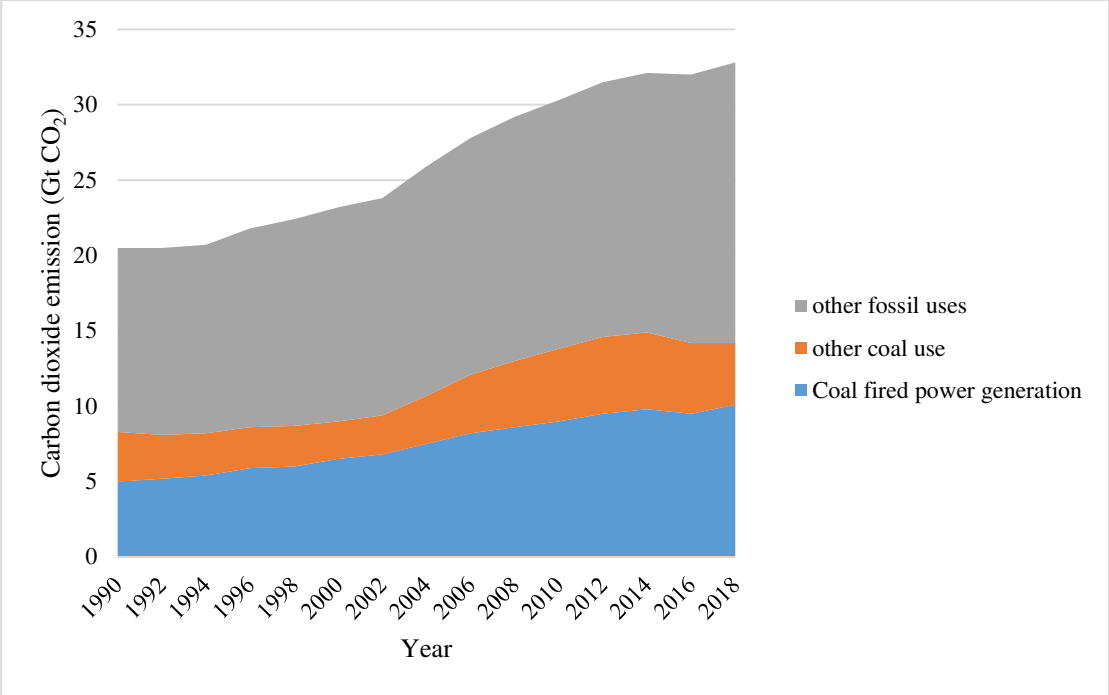

Fig 1.3: Global carbon dioxide emission by different sources, 1990-2018 [7].

Fig 1.4 shows that change in global CO_2 emission was very less in 2014 but in 2015 and 2016 it became negative and in 2017 & 2018 it increased by huge margin.

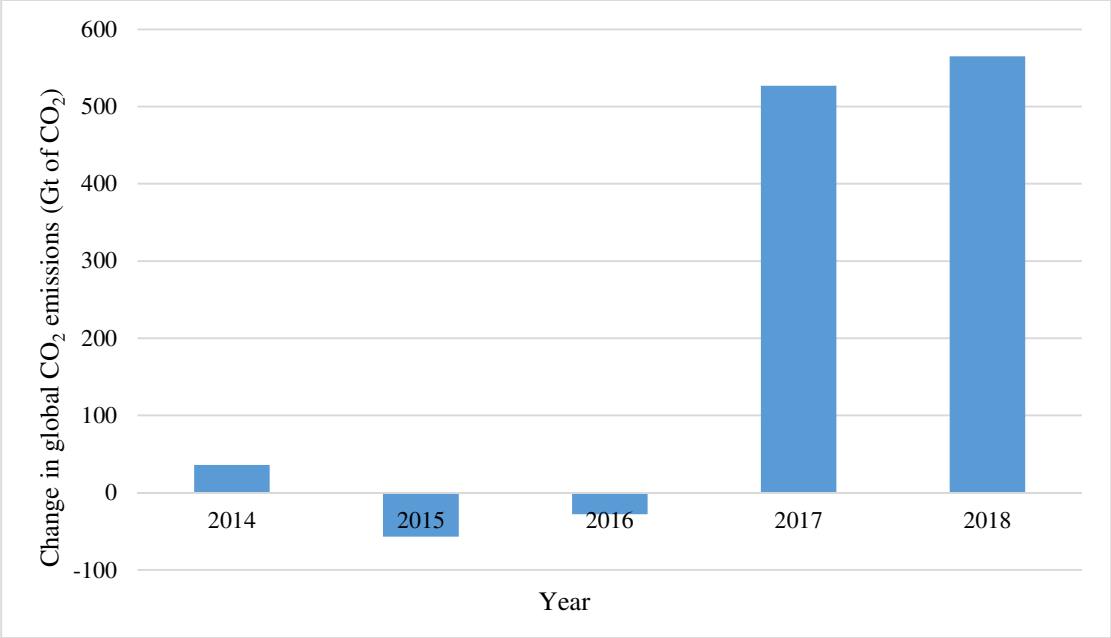

Fig 1.4: Change in global carbon dioxide emissions. 2014 -2018 [7].

1.2 INDIA'S ENERGY SCENARIO AND FUTURE OUTLOOK

1.2.1 *India's Electricity generation mix and Future outlook*

India is set for a huge shift as Government of India has laid out some developmental ambitions as follows:-

- 175 GW installed capacity of renewable energy by 2022.
- 24 × 7 power for all by 2022.
- Housing for all by 2022.
- Mission of building 100 smart cities.
- Transitioning and availability of clean cooking fuels.
- Meeting the INDC targets as committed in COP 21 Paris.

India is anticipated to play a pivotal role in global energy scenario among the current trends which are favoring the energy buyers rather than energy suppliers which is likely to continue for a good term. India is likely to contribute 25% of the rise in global energy demand by 2040 [8]. India's energy demand is expected to be rising at a CAGR of 3.7% - 4.5% and electricity demand at a CAGR of 5.4% - 5.7% till 2047, the pressure on natural resources as a fuel is forecasted to grow in future at a rapid rate. With India accounting for 18% world's population, India's consumption of energy is only 6% of world's primary energy consumption, the reason behind is the low per capita energy consumption which is about one-third (1149 kWh per capita for India) of world's per capita energy consumption. India surely will try to elevate its low per capita energy consumption through sustainable methods keeping in mind the impact of these targets on economic growth.

The energy mix of World and India are shown below in Fig 1.5 and Fig 1.6 respectively. From analyzing the data of electricity generation mix of India and World, it can be seen that there is not much difference except the share of coal i.e. 75.9% and 38% respectively whereas the hydro and other sources contributes about 11.3% and 19% in India and World respectively. Also there is a lot of scope and potential of Solar based energy generation

in India which needs to be explored so that India can reduce its realization on fossil fuel based energy generation.

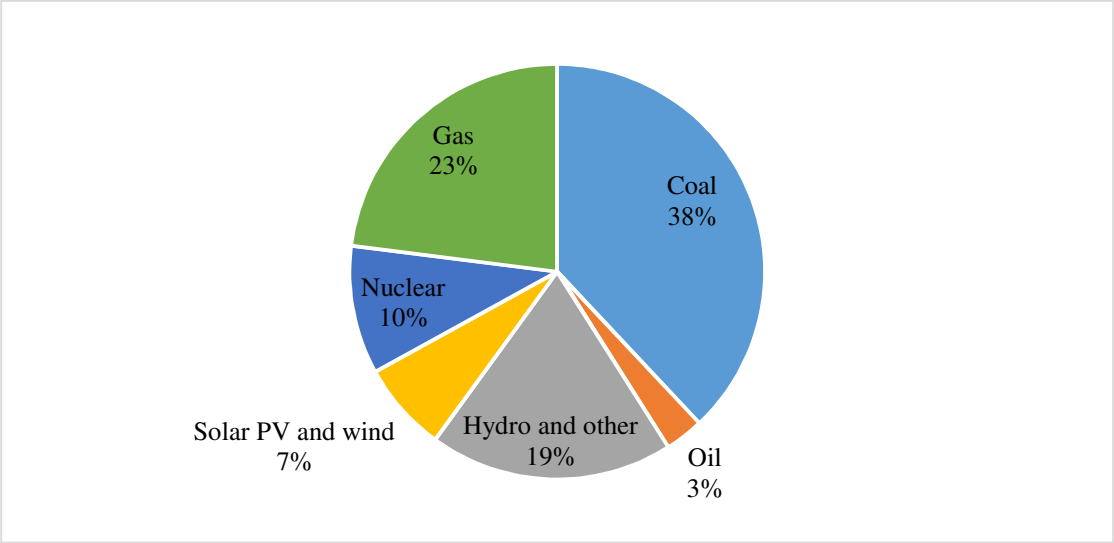

Fig 1.5: Electricity generation mix of world 2019 [7] (As on 1 August 2019).

India's energy sector is largely dominated by fossil fuels, especially coal. During 2017-18 fiscal year, energy generated by coal was two-thirds of the total energy produced approximately 75.9% share. However, Government of India is trying to push the investment and electricity generation by renewable sources of energy. Also in The National Electricity Plan 2018, drafted by GOI, says that country does not need any additional conventional fuel based power plants.

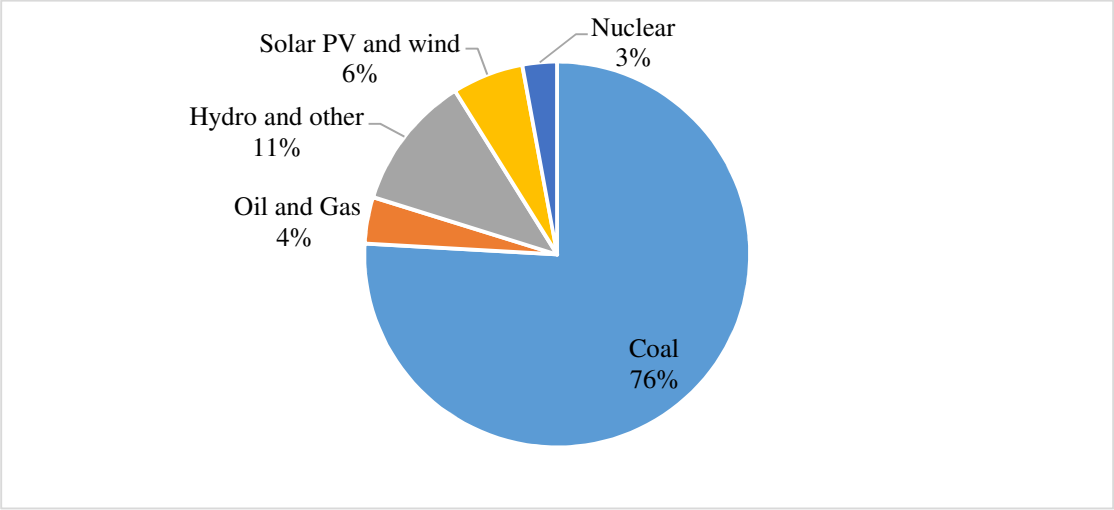

Fig 1.6: Electricity generation mix of India 2019 [9] (As on 1.August.2019).

1.2.2 *India's power sector at glance*

Table 1.1: Total installed capacity [10] [11] (as on 31/07/2019).

SECTOR	Megawatts	Percent of total
State	90,177	25%
Central	102,818	28.5%
Private	167,462	46.5%
Total	3,60,456	

Fuel	Megawatts	Percent of total
Total Thermal	2,27,644	63.2%
Coal	1,95,810	54.3%
Lignite	6,260	1.7%
Gas	24,937	6.9%
Oil	638	0.2%
Hydro	45,399	12.6%
Nuclear	6,780	1.9%
RES	80,633	22.0%
Total	3,60,456	

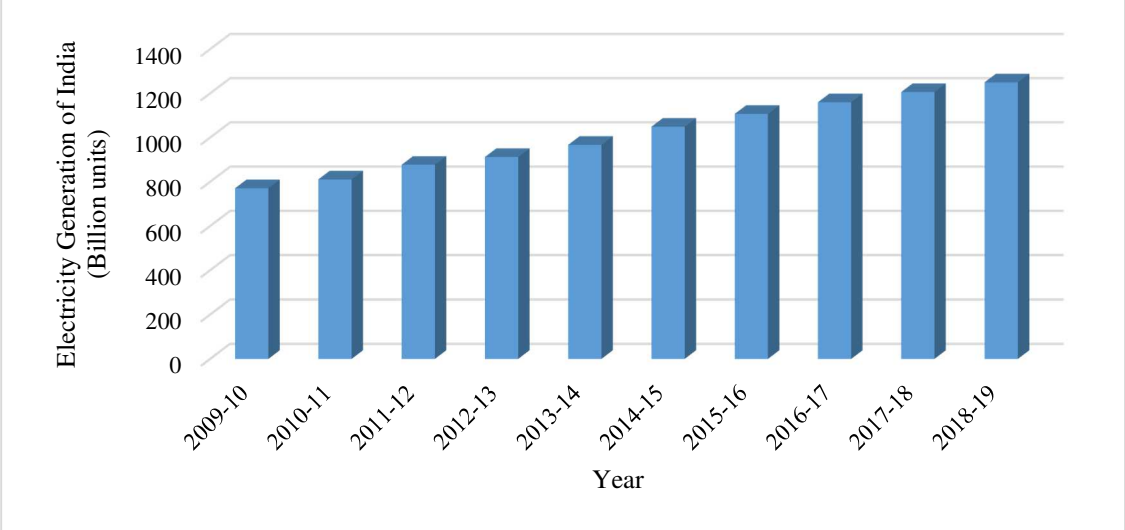

Fig 1.7: Generation of electricity in India (in billion units) 2009-19 [11].

Fig 1.7 shows the trend of electricity generation of India in billion units. It shows that there is a gradual increase in electricity generation over the past 10 years from 2009-2019

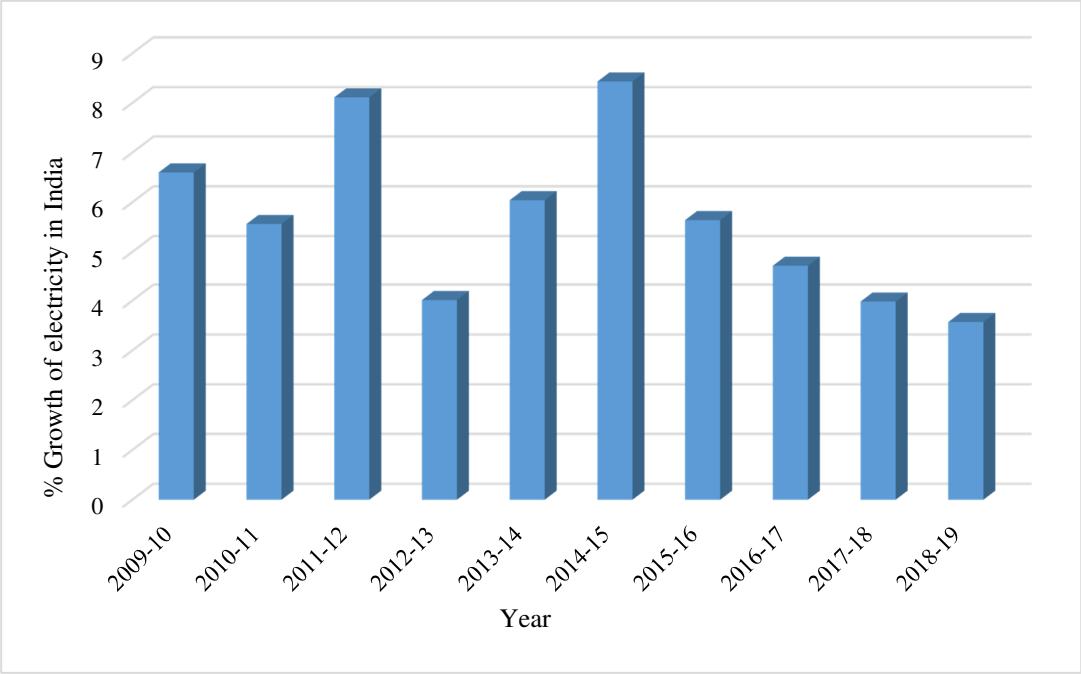

Fig 1.8: Generation growth of electricity in India (%) 2009-19 [11].

Fig 1.8 depicts that there is decrease and then increase in % growth of electricity from 2009-2012. From 2012-2015 there is rapid increase and then followed by continuous decrease in electricity generation growth from 2015-2019.

1.2.3 *Renewable energy scenario in India*

India has shown a positive outlook for encouraging production and demand and supply of renewable energy sources over a long period of time. Along with the grid power, distribution of electricity generated through renewable energy offers an efficient way to meet rural India's heating, lighting and other energy use.

In 2015, Government of India had announced to achieve the target of total installed capacity of 175 GW by the end of 2022. India also possess decent world ranks in wind power deployment and solar power deployment as 4th and 6th respectively.

Renewable energy has a vital to play role in driving India towards the path of augmentation of power grids, less fossil fuel consumption and low carbon emission.

Before commencement of COP-21, India has drafted its INDC to UNFCCC, mentioning the actions to be taken after 2020 climate related steps. India is also determined to reduce its GHG emission per unit GDP by 33% - 35% below the levels of 2005 by 2030, and also to establish the carbon sink of about 2.5-3 billion tonne of carbon dioxide through planting a huge number of plants. India also launched the NSM in 2010 under NAPCC which initially aimed to install 20 GW grid connected solar power plants to be achieved by 2022, which was later increased to 100 GW for the same target year.

Table 1.2: Achievements in grid connected renewable power [12].

Source of energy	Cumulative achievements (Megawatts) (As on 31/12/2017)
Wind Power	32848.46
Solar Power - Ground mounted	16070.07
Solar Power - Roof Top	982.30
Small Hydro Power	4418.15
Bio Power	8413.80
Power (from waste)	114.08
Total	62846.86

Major Achievements of India's Renewable energy sector are mentioned below:-

- India's global ranking of wind energy installed capacity is 4th.
- There were decline in wind and solar tariffs due to competitive bidding, as low as Rs 2.44/kWh in case of wind tariffs.
- Kurnool Solar Park has been commissioned in Andhra Pradesh with 1 Gigawatts capability, making the park the largest solar park in the world.
- Capacity of 650 Megawatts commissioned in Rajasthan's Bhadla phase 2 Solar Park and also capacity of 250 Megawatts installed at Phase 1 Solar Park in of Neemuch Mandsaur, Madhya Pradesh.

- In FY 2017-18, a total of 72 nos. of 2208 Suryamitras services are organized under the Suryamitra Program.
- Projects worth Rs 6766 Cr were granted under the Green Energy Corridor project and also Rs 1400 Cr form the Government of India's share were disbursed to the states.
- 32649 irrigation and drinking water solar pumps have been built and 20125 biogas plants have been installed.
- The National Offshore Wind Policy recognizes India's offshore wind potential.

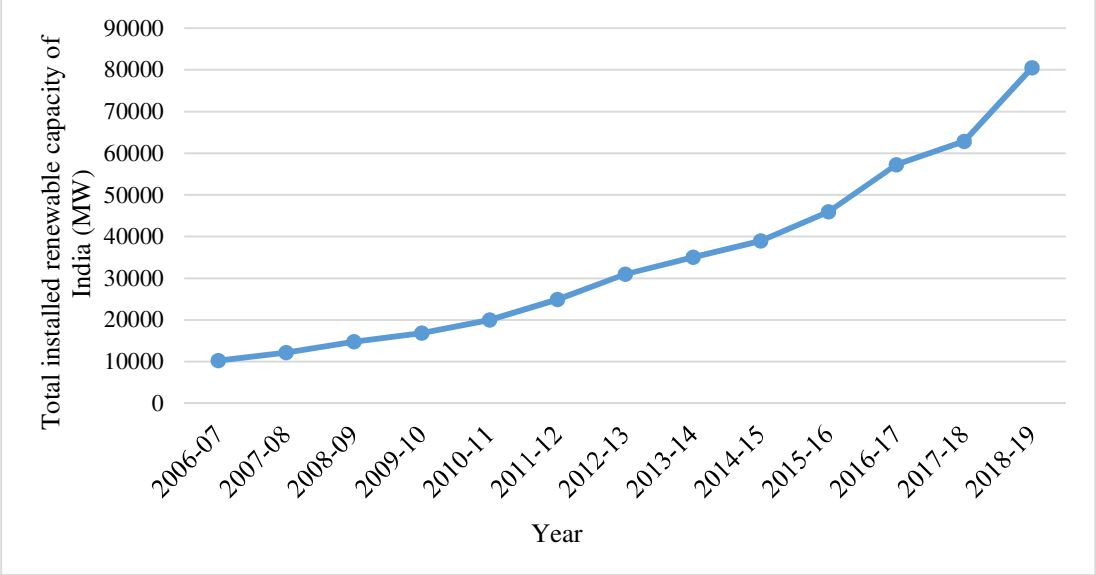

Fig 1.9: Total installed renewable capacity of India 2006-19 (MW) [12].

In Fig 1.9 it is observed that from year 2006-07 to 2011-12, there is gradual and continuous growth of installed capacity of renewable. Total installed renewable capacity (MW) as the demand increases, there is exponential growth of installed capacity from year 2012-13 to 2018-19. As the conventional source of energy is diminishing and are a threat to environment, India is shifting towards the renewable source of energy by installed renewable power plant. Fig 1.10 shows that trend that from 161 MW installed capacity of solar PV in 2010, India has now cumulative installed capacity of solar PV of 28181 MW in 2019.

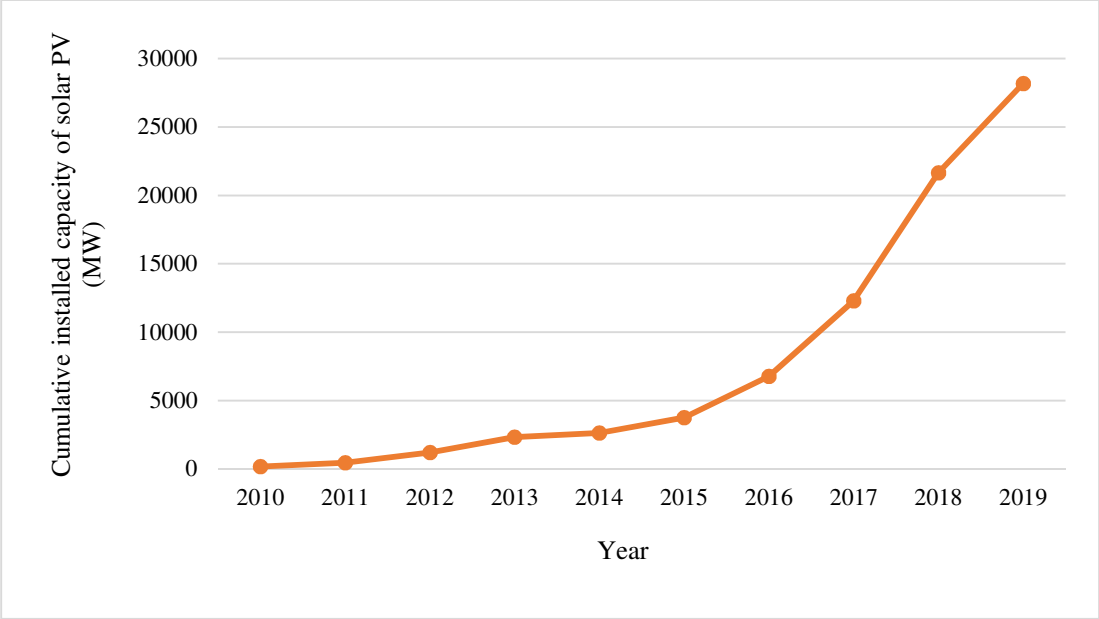

Fig 1.10: Cumulative Installed capacity of Solar PV of India, 2010-2019 [12] (As on 31 March 2019).

1.2.4 *SOLAR ENERGY POTENTIAL IN INDIA*

India is home to an exceptional range of climatic areas, from tropical areas from south to temperate and alpine regions in the middle of the Himalayas, where high areas receive continuous winter rainfall. Since India's climate is mainly controlled by the Himalayas and the Thar dessert. There are approximately 300 sunny days annually so there exists a significant Solar Energy potential which can be trapped to generate large amount of electricity. The solar energy potential of top 5 states of India are Rajasthan (142.31 GWp), Jammu and Kashmir (111.05 GWp), Maharashtra (64.32 GWp), Madhya Pradesh (61.66 GWp), Andhra Pradesh (38.44 GWp).

1.3 *SOLAR CHIMNEY POWER PLANT (SCPP)*

India is a developing country where each industry is growing at high pace, such as automotive, process automation, estate and agricultural. As each industry grows at a fast pace, they face a significant power supply issue. The current generation of electricity is lower than the demand supply needed so they must shut down their power generating units for a day or two to balance the power distribution which will result in slowdown of

Indian economy. Maximum power generation in India is based on fossil fuel which will not last for a long time and also they affect our climate and environment. So there is need to switch to renewable source of energy, largely on Solar Power Energy. In India, the geographical location and fixed seasons are best suited for solar power plants that give insight into solar chimney energy plants [13].

1.3.1 *WORKING PRINCIPLE OF SCPP*

Fig 1.11 shows the basic details of the SCPP. It comprises of Solar chimney, Solar collector, Turbine. SCPP helps to convert solar radiation into electricity. Direct and diffuse solar radiation falls on the solar collector where, owing to the environment, clouds and climatic condition, particular fraction of energy is reflected back, transmitted and absorbed. The quantity of reflected, absorbed and transmitted energy depends upon the angle of incidence of solar radiation and the optical characteristics of the material of collector surface such as refractive index, thickness, thermal conductivity etc. [13].

The solar radiation transmitted through the collector roof strikes the ground where the portion of the radiated energy is absorbed by the surface and some portion is reflected. The reflected fraction of the radiation warms up the air under the collector. Hot air (lower density), due to the density difference, moves up to the plant's chimney [14]. It results in empty volume under the collector roof which is rushed by the ambient cold air (higher density) which establishes the forced convection air circulation. As the air moves from the collector periphery through the chimney, its temperature rises but the air velocity is approximately constant throughout the stack because the stack's height is less. The heated air moves up creating the pressure difference at the chimney inlet and outlet so that the air flowing through the chimney drives the turbine to generate the electricity [16].

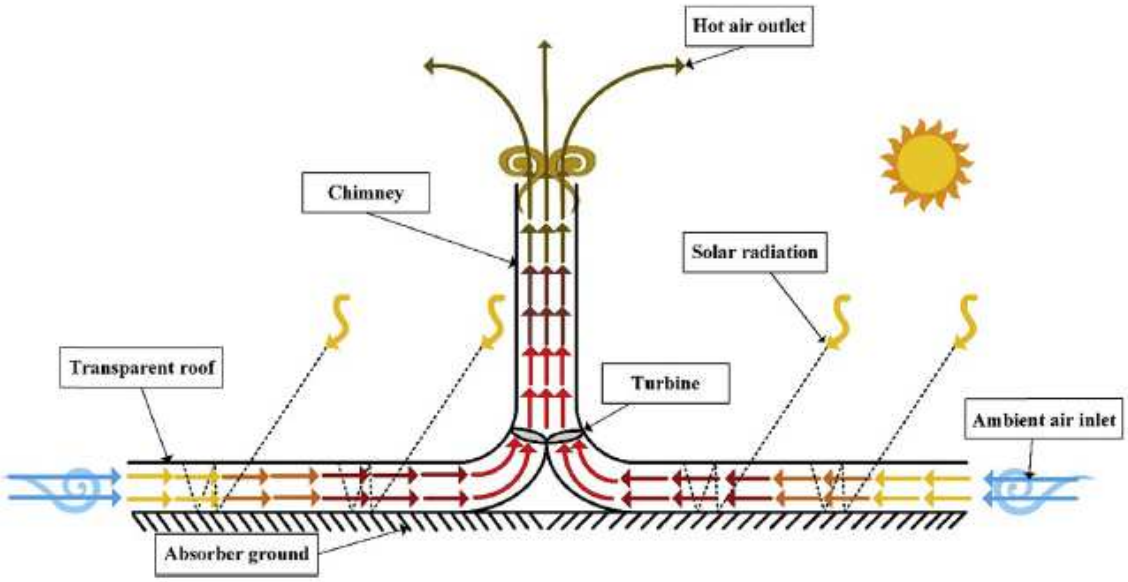

Fig 1.11: Schematic diagram of SCPP [15].

1.3.2 BASIC COMPONENTS OF SCPP

There are 3 vital components of SCPP as follows:-

1. Solar Collector

Solar Collector is the primary component of the SCPP. Solar energy collectors are the special type of the heat exchangers that transform solar energy into the transport medium's internal energy [17]. Collector establish the greenhouse effect which heats up the inlet air. The collector's radiation is used to warm up the air inside the canopy [18]. The material used for construction of solar collector is PVC sheet of 0.5 mm thickness. The solar collector roof is sloped at an angle of 28.75^0 (latitude of location of SCPP model setup). The quantity of radiation received relies on the collector's material and the solar radiation angle.

2. Solar Chimney

Another major component of the SCPP is solar chimney. SCPP efficiency relies on the chimney's material, surface, and height of chimney, tapered angle, and chimney's diameter. It is installed in the solar collector's roof centre. Hence the temperature

difference between the inlet and outlet of the stack will help the air to move up through the wind turbine. The upward motion of hot air is used to drive the turbine in the chimney. For the proper flow of air, minimum friction losses and maximum utilization of air, the turbines are mounted at the center of the solar collector. Efforts to improve the effectiveness of the SCPP sloping solar chimney, hybrid drying solar chimney is used. In our model, height of chimney is 1250 mm and outer and inner diameter are 207 mm and 205 mm respectively.

3. Turbine

Turbine is an integral unit of SCPP which converts the air flow energy into the mechanical energy and transmits it to the generator. It resembles the wind turbine and situated at the bottom and inside solar chimney. The velocity of the turbine owing to the air flow allows the generator to produce and power it to the grid [18], [19]. In order to obtain maximum power from hot air, turbine blades should cover complete cross sectional area of base of chimney. In experimental setup, turbine is replaced by the inlet duct fan.

1.3.3 *MERITS OF SCPP*

1. It is especially appropriate for arid regions and sun rich waste land.

2. It generates electricity 24 hours a day if heat transfer medium can be accommodated which absorbs the heat during day time and provide thermal energy during night time such as molten salt, supercritical CO_2.

3. It does not demand any fuel to work therefore saving the cost of fuel as compared to conventional sources of energy.

4. There is no need of cooling water which makes it useful in the dry and arid regions where there is water scarcity.

5. Since it works on renewable source of energy and there is no emission during the electricity generation, so it does not have harmful impact on the environment.

6. SCPP is very low maintenance because there is only one moving equipment that is turbine. Also there is maintenance for cleaning of the solar collector surface which is not done frequently.

1.3.4 *DEMERITS OF SCPP*

1. SCPP requires a large collector area to setup the plant.

2. High setup and construction cost.

3. It has efficiency of order 0.1%

4. High tariff rates for electricity.

CHAPTER-2

LITERATURE REVIEW

This chapter deals with Solar Chimney Power Plant and Solar Dryer Thermal Efficiency & Exergy Analysis literature. Also, it further discusses the objectives and research gaps of this project work.

2.1 *Literature survey*.

Hu et al., [20] performed numerical simulations and analyzed solar power chimney performance with divergent chimney by considering two form control parameters which are first one is the chimney exit area ratio above the entrance and second one is the angle of divergence. The divergent chimney can produce higher power output compared to the traditional cylindrical chimney. This increase in power output initially increases and then decreases as the area ratio increases and the angle diverges. In addition, the parametric studies show that both the shape influencing parameters have different effects on the power output increase: the area ratio can have a dominant effect on the enhancement effect and the divergent angle can have a dominant effect on the rate of change of enhancement effect. The performance analysis of the divergent chimney was observed on the 1st group configuration of height and area ratio, that is, solar chimney power plant having chimney height as high as 200 meters and area ratio in the range of 1.25 to 32. Cylindrical chimney numerical tests were taken as our reference or normal scenario. As the results suggest, the energy output of the SCPP with divergent chimney could clearly increase. Therefore, the efficiency of the solar chimney power plant has a positive effect on the increase in power output. When area ratio is increased to 10, the power output increases and reaches a peak of 13 times that of the benchmark (cylindrical chimney) scenario. In fact, when the area ratio is increased, the power output tends to decrease, which may be due to the isolation of the boundary layer at the chimney wall. In the case of a divergent chimney system, the temperature variability has much less effect compared to the other variables. The temperature difference rises to 21.4 K for the cylindrical chimney, while the temperature difference rises to 12.4 K for the divergent chimney. Although the lower temperature appears to decrease the driving potential, the main factor

for increased driving potential in the case of the divergent chimney system is the divergent form of the chimney which acts on the pressure recovery mechanism. By considering several chimney heights, various effects of Area Ratio and Divergent Angle on the output of the SCPP are observed. The result found is that the area ratio controls the enhancement effect and divergent angle controls the enhancement effect change frequency.

Abdelmohimen et al., [21] conducted a statistical survey of the quality of SCPP with a chimney height of 194 meters and a collector diameter of 244 meters capable of producing an average of 56 kilowatts per month over the year in the city of Riyadh. The peak power production in the Bisha region of Saudi Arabia is also found to be 63 kilowatts. There are two variables i.e., solar radiation and atmospheric temperature quality that affects SCPP. And the output of the collector ranges from 10% to 29% throughout the year. Six separate locations in Saudi Arabia are selected to test the quality of SCPP. The average monthly solar radiation levels have been used to calculate the average monthly power generation. According to this article, the maximum solar radiation occurs in different locations in Saudi in springs and summers. During winter, in the cities of Bisha and Jeddah, the maximum solar radiation drops. According to NASA's last 22 years of average temperature and monthly solar radiation results, the hottest summer cities are Riyadh and Hafar Al-Batin, while Jeddah is the hottest city in other months. Tabuk and Jeddah generate a maximum power output of 84.5 kilowatts and 83.1 kilowatts respectively in June. The two important factors influencing power generation are solar radiation and ambient temperature. These two factors listed cannot be interpreted independently because in different locations they are interdependent on each other. Generally speaking, as solar radiation increases at a particular location, power production and collector efficiency tend to increase. This paper concludes the analysis of the numerical model and validates the findings with the experimental data.

Xu et al., [22] simulated the DSPP and analyzed DSPP output by adjusting the COAR across a wide range of values. Studies show that as COAR increases, the propensity to split the boundary layer (BLS), stream stall, back flow, vortex formation increases. Due to the low ambient temperature water, the temperature above the separation point of the boundary layer would decrease significantly, resulting in a significant decrease in the

buoyancy effect in the divergent chimney. The pattern of COAR vs. TPP is that when COAR increases, TPP increases and at COAR=8.7 reaches a maximum value. With COAR's further rise, TPP would begin to decline. At COAR=8.7, the maximum output of 231.7 Kilowatts is also achieved, which at COAR=1 is approximately 11.9 times. The area of blocked cool air flow increases with COAR and height over the separation point of the boundary layer.

Najm et al., [23] done mathematical computation of the efficiency and power generation of the solar collector and numerical simulations indicate that the radius of the solar chimney collector is optimum and dependent on global solar radiation. The effect of a decrease in turbine pressure on the optimum radius is also significant. The optimum collector diameter will increase as the turbine pressure drops. The optimum radius of the solar collector at the turbine pressure drop of approximately 160 Pascal and 500 W/m^2 global solar radiation is about 17 times. The air temperature increases significantly by increasing the collector diameter and global solar radiation. In the case of 72 meter collector radius and 900 W/m^2 solar irradiance, the stored internal energy is comparatively higher compared to 172 meter solar collector radius and 300 W/m^2 solar irradiance. Increasing the diameter of the collector increases the transfer of heat to water. The ideal solar collector radius achieves full collector output. Also, the solar collector diameter will further increase and the collector output will decrease. The air mass flow rate is largely dependent on the diameter of the solar collector rather than the height of the plate. If the stack height increases from 175 meters to 215 meters with global solar irradiance of 500 W/m^2 and maximum radius, the turbine output power rises by approximately 19% and insignificant effect on collector efficiency. At 72 meter collector diameter, 195 meter stack height and 500 W/m^2 solar irradiance, increasing the surrounding temperature from 293 K to 323 K, the solar collector efficiency rises from 77.8% to 82.3%. To achieve the optimized solar collector output, the maximum pressure drop of 100 Pascal inside the wind turbine is recommended

Fadaei et al., [24] conducted an experiment and studied latent heat storage in SCPP with and without PCM and its effect on various parameters such as air speed and temperature. The material used in this experiment was paraffin wax. Paraffin wax increased the thermal

efficiency with the latent heat storage system. Since there is use of the material for phase change, the intermittency issue is also solved. Because of the use of solar chimney with phase change material, the total air velocity is increased by around 8.33%.

Fathi et al., [25] suggested using nuclear power plant waste heat to increase SCPP air temperature, which may in turn reduce the combined cycle value. The combined cycle thermal efficiency depends on the ambient temperature. The combined cycle thermal efficiency can be increased by 8.7 percent, which has a major impact on the cost of capital. A combined cycle is best suited for arid regions because water cooling does not require a separate unit. The efficiency also tends to increase at night and this improvement is sustained up to 4 percent. The cooling water distribution system and intermittent power supply have been replaced by this novel idea.

Jafarifar et al., [26] investigated the impact of ambient crosswinds on indoor air speed and SUT performance. This found the place with low solar irradiance and high ambient air crosswinds and compared it to the place where, through numerical modeling analysis, there are not so intense crosswinds. The results are that SUT's internal air speed and efficiency can be improved by 15 percent and 50 percent respectively by ambient air crosswinds. The results show that if the impact due to the ambient is overlooked and the lower solar irradiance is considered then the internal air speed will be significantly reduced by about 33% and the SUT output will be reduced by about 53%. Thus even the lower solar irradiance is considered then the loss of SUT output can be balanced by the effect of strong crosswinds.

Amudam et al., [27] analyzed the numerical 3D model and examined the impact of the thermal storage device on the power plant of the solar updraft building. The parameters taken into account for two different models without (Model-1) and with (Model-2) thermal energy storage system are temperature, velocity, pressure and density. Sand rock mixture is known as the processing medium for thermal energy. The experimental results show that the result value for Model-2 is lower compared to Model-1 considering collector capacity, overall efficiency, power output, because there is some heat absorbed by the thermal energy storage system. For both the model and the maximum pressure drop position, the pressure decreased between the inlet of the chimney and the

atmosphere, i.e. 81.9 Pa in Model-1 and 73.72 Pa for Model-2. The Model-1 chimney's peak air velocity was also 6.8 m/sec and Model-2 was 4.24 m/sec. The maximum temperature observed for Model-1 was 308.5 K and Model-2 was 306.53 K and location of highest temperature was at the stack.

Hassan et al., [28] performed a parametric 3D CFD study to determine the effects of the slope of the collector and the divergent angle of stack / chimney. The numerical model was investigated using DO, solar loads and system k- RNG. Consistent with all other considerations, numerical simulations were performed at various collector slope values of 4^0, 6^0, 8^0, 10^0 and stack divergent angle of 1^0 - 3^0. Based on the findings, as the slope quality of the collector was increased, both air temperature and air velocity were increased due to higher heat transfer and mass flow rate but The development of vortices and air stagnation occurs at a collector's slope value greater than 6^0 due to the recirculation of air hamper resulting in a decrease in overall efficiency. In the chimney divergent angle = 1^0, the air velocity value rises dramatically from 9.1 m/sec to 11.6 m/sec, resulting in a 108% increase in output power

Balijepalli et al., [29] measured the solar updraft tower with a collector diameter of 3.5 meters and a chimney diameter of 0.6 meters. The results show that the average air velocity inside the stack was 2 m/sec, the maximum output was 0.633 watts and the maximum overall efficiency was 0.0028 percent. The results show that the average air velocity inside the stack was 2 m/sec, the maximum output was 0.633 watts and the maximum overall efficiency was 0.0028 percent. Rocks are known as the material for thermal heat processing. The average decrease in the chimney pressure was 1,065 N/m^2. Model measurement was also done to find out the turbine blade's optimum chord size. GFRP is the material used for the turbine rotor blade because it has properties such as light weight, higher thermal strength and can work better under static and dynamic forces than other materials.

Cottam et al., [30] evaluated the thermodynamics of the solar chimney collector of steady state analytical model. The effect of different canopy designs is also evaluated. It also displays the maximum power output being measured at different dimensions and different forms of canopy profiles. Results showed that the canopy height has a very

significant effect on the power plant of the solar chimney. The canopy must be mounted at significant height around the junction of the chimney to achieve the maximum kinetic energy of air at the inlet of the solar chimney. The canopy layout can also be constructed in the stepped annular flat sections for easy manufacturing. It concentrated on three forms of canopy profile, i.e. straight, sloping with steady gradient and exponential. The flat canopy profile is simple in terms of manufacturing and design, but major pressure losses occur due to air flow restriction. It is seen that sloping canopy layout with constant gradient can help achieve better thermal performance of the SCPP. The exponential model could increase the plant's output nevertheless, its development, production and maintenance are complex, which also increases the cost of capital. The canopy outlet height found to be the essential parameter which indicates the fall in flow pressure at the junction of the collector and chimney. The segmented canopy results profile shows approximately the same power output as the exponential canopy model.

Mehrpooya et al., [15] solved a three-dimensional (3D) SCPP model for Tehran climate data using CFD process. The geometry of the model is taken from the Manzanares SCPP prototype. Comprehensive analysis of chimney mathematical equations, transparent roof, storage surface, and other SCPP elements. The key parameters of the SCPP model for Tehran city 216 climate data points were examined to check the model's validity. The performance analysis with surface temperature variance and average heat coefficient of conduction is performed. In addition, the energy and exergy research approaches analyze the thermodynamic understanding of the entire SCPP system. The findings of the sensitivity analysis show that the production energy varies from 180 W in the winter nights to 64 kW in the summer noon by variance of the solar radiation. In this scenario, the efficiencies of energy and exergy range from 3.50 percent to 93.3 percent and 2.00 percent to 29.0 percent respectively.

Prakash et al., [32] planned, constructed and examined modified greenhouse dryer the effect of coefficients of h_{cv}, heat loss, C_{df}, and the factor of instant thermal loss efficiency. With the support of a mirror, the north wall is translucent to reduce the losses. Two sets of tests have been carried out. Firstly, the barren ground condition and secondly, the

barren ground was covered with black sheet. The constant C and exponent n are determined using regression analysis from the experimental data.

Dev et al., [33] used the characteristic function to produce linear and non-linear characteristic equations for different season conditions for experimental results of a passive solar still. For both winter and summer conditions, the different angles of inclination of the condensing cover (15^0, 30^0, and 45^0) were chosen. It was observed that the still 45^0 inclined passive solar gives better output in both winter and summer. In summer weather conditions, different water depths (0.04 m, 0.08 m, 0.12 m and 0.16 m) were also taken for solar still with a 30^0 angle of inclination. Instant gain and loss efficiency correlations at water depths of 0.01 and 0.04 m for slope of 15^0 were also designed to determine the overall effect of height of water level on efficiency of solar still. In order to provide greater efficiency, a lower water depth was identified, resulted in accordance with many scientists. Instantaneous efficiency curves were concurrently measured to provide a good grasp of the productivity of solar still. The suggested solution will be used to optimize the design and maximize the power production.

Prakash et al., [34] assessed MGD in active mode (AM) and passive mode (PM) for annual performance, environmental analysis, energy & exergy computation. Thermal treatment is applied to the surface of MGD. It's achieved in three specific ways: bare ground, covered floor with black PVC and black coated floor. Under no-load conditions, experimental analysis of greenhouse dryers shows that floor covered with a black sheet of PVC is better than other floors conditions. MGD under Active is more active than tomato and capsicum under Passive mode, which are highly moisturized crops. Both dryers demonstrate relatively similar drying quality for a plant containing moderate humidity (potato chips).In the greenhouse dryer, result shows that dried crops are more nutritious than dried open sun crops. The adjusted greenhouse dryer's payback period in passive mode is 1.11 years. But the adjusted greenhouse dryer's active mode is only 1.89 years. The dryer's passive mode's embodied energy is a 480.277 kilowatt hour and 628.73 kilowatt hour for the dryer's AM. The annual CO_2 emissions for greenhouse dryers in passive and active mode are 13.45 kilogram and 17.6 kilogram respectively. The period for energy payback, carbon reduction and carbon credit are calculated based on dried

plant size. The HUF variance for MGD under passive mode is 0.12–0.38 and 0.26–0.53 for MGD under active mode. The performance coefficient (COP) varies for MGD under PM as 0.55–0.87 and MGD under AM as 0.58–0.73.

Chauhan et al., [35] planned, manufactured and tested the modified greenhouse dryer for natural convection condition under no-load. For 2 different type of cases, Case 1 and Case 2, tests are performed. Case 1 was a greenhouse dryer enclosed and insulated by the north wall with a solar collector on the floor and Case 2 is a greenhouse dryer enclosed and insulated by the north wall without a solar collector. Performance indicators as h_{cvt}, C_{df}, Q_{lf}, power utilization factor and efficiency coefficient were evaluated and analyzed for newly developed process. The total output coefficient value for Case 1 was 0.9 while for Case 2 was 0.86. For Case 1, the maximum heat usage factor was 0.68, while for Case 2, 0.61. The largest temperature differential for the greenhouse dryer with the solar collector between indoor air and outdoor air was 30^0 C, 28^0 C and 18^0 C respectively for day 1, 2 and 3 respectively. The temperature of the indoor air in the room was 46%, 42% and 32% greater than the temperature of the ambient air in day 1, 2 and 3 respectively. The results confirms the alternate modified process. So the device established for fruit / vegetable drying is recommended.

Kumar et al., [36] constructed a thermal model to forecast jaggery temperature, greenhouse air temperature and evaporated moisture, while drying jaggery under natural conditions of convection. For full drying, the test was carried out separately for 0.75 kg and 2.0 kg of jaggery parts with measurements of 0.03 x 0.03 x 0.01 m^3. In a roof-type span greenhouse with floor area of 1.20 x 0.78 m^2, the jaggery was dried. The experiment was conducted at IIT Delhi (28^0 35' N 72^0 12' E) from 10 a.m. to 5 p.m. on February 5–8, 2004. MATLAB software developed a computer program to measure the jaggery temperature, the temperature of the greenhouse air, and the evaporated moisture and based on solar intensity and ambient temperature, predict greenhouse thermal performance. The code developed has been tested experimentally. It has been shown that there is good agreement between the analytical and experimental findings for jaggery drying. The thermal model developed in this paper was validated with the experimental observations. The predicted values and experimental measurements were in good

agreement with the jaggery and greenhouse air temperature correlation coefficient varying between 0.90-0.98 and 0.96-1.00 for the jaggery mass during drying.

2.2 *Research gap*

Ongoing through the research work involving the study of the SCPP, it has been found that very limited work has been done regarding the system of SCPP and solar drying. Also there is limited discussion regarding the influence of parameters like convective heat transfer coefficient, exergy analysis, and divergent angle of chimney, area ratio of chimney and incorporation of thermal energy storage system for system of SCPP with solar drying. These parameters tends to increase the performance of the SCPP.

2.3 *Objectives*

Based on literature review, following are the objectives of this research.

- To evaluate of thermal performance parameters; convective heat transfer coefficient, COP, HUF.
- To develop the performance characteristic curve and characteristic equation for SCPP with solar dryer.
- To perform exergy analysis for SCPP with solar dryer.

CHAPTER-3

METHODOLOGY

This chapter focusses on the methodology used to perform the experimental work and to evaluate the various parameters. All the input parameters and data, method and process and numerical computation that has been used during the course of this project work are discussed in details.

3.1. *Experimental setup*

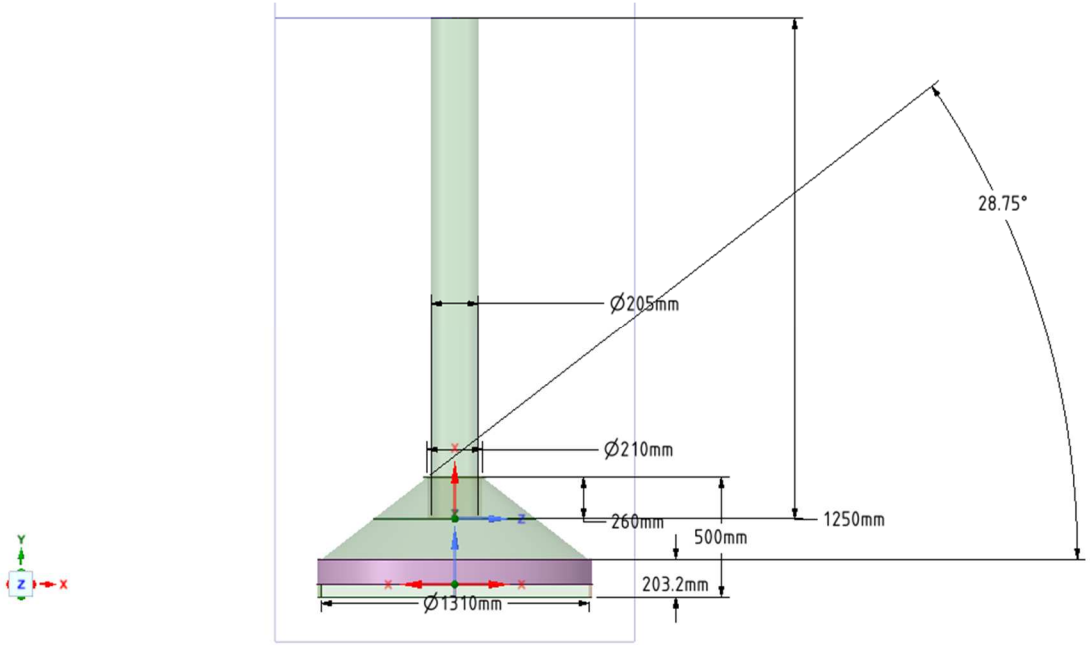

Fig 3.1: Dimensional line diagram of SCPP model used for experimentation.

The dimensional and material details of experimental model of conventional cylindrical type solar chimney power plant is provided below.

The dimension of SCPP experimental model was taken into account by keeping in mind the space constraint and ease of manufacturing. Also the model was designed using SPACE CLAIM (ANSYS). Solar chimney is made up by cold rolling of mild steel sheet having total height of 1250 mm, outer diameter 207 mm and inner diameter 205 mm which is supported by a stand, made up of steel, having height of 500 mm. The basic structural frame for solar collector is made up of iron billets having effective clearance

from ground of approximately 76.2 mm. Solar collector is generated by wrapping PVC sheet of thickness 0.5 mm around the basic structure and is used to create the greenhouse effect by transmitting solar radiation.

Table 3: Dimensions of different parameters of SCPP experimental model.

S.No.	Parameter	Dimension
1.	Chimney height	1250 mm
2.	Chimney inner diameter	205 mm
3.	Chimney sheet thickness	1 mm
4.	Collector/canopy top diameter	210 mm
5.	Collector/canopy bottom diameter	1310 mm
5.	Canopy height	296.8 mm
6.	Chimney support stand height	240 mm
7.	Drying tray effective area	0.2903 m2
8.	Canopy clearance from ground from bottom diameter	76.2 mm
9.	Canopy clearance from ground from top diameter	500 mm
10.	Collector slope angle	28.750

Solar collector is sloped at an inclination of 28.75^0 (Location of DTU- 28.75^0 N, 77.11^0 E) to harness the maximum solar incident radiation. The diameter of solar collector is

1370 mm. The drying tray (4 in no.) is used to dry out fruits, crops etc. have total effective area of 0.2903 m^2. For enhancing the power output, vents in 4 direction are also been made for the smooth flow of air inside the canopy. An inlet duct fan is placed inside the chimney at chimney inlet having maximum rpm of 3000, 6 blades. It represents the wind turbine which is coupled to generator to generate the electricity in a working SCPP.

Fig 3.2: Experimental model of SCPP along with the instruments used.

3.2. *Equipment*

Solar power meter (digital) measured the incoming solar radiation which falls on the sloped solar collector. System air relative humidity was measured by using thermo-hygrometer. Ground temperature and system temperature were measured with the help of K-type thermocouple and 12 channel temperature indicator. Wind velocity at inlet and outlet was measured by using vane type anemometer. The detailed specification of the instruments are given in Table 4.

Table 4: Specifications of measuring instruments.

S.no.	Measuring Instruments	Specifications
1.	Inline Duct Fan	Diameter: 8 inches
		Material: ABS + Steel
		Fan speed: 3000 rpm
		Voltage: 220 V
		Power: 12 W
2.	Solar Power Meter	Sensor: Extra Sensitive Silicon Photodiode
		Spectral Response: 400~1100 nm
		Range: 0~2000 W/m (0~ 634 BTU / ft .h)
		Accuracy (at 23°C, 60% RH): ±10W/m (±3 BTU/ ft .h) or ±5% (whichever is greater)

		Resolution: 0.00~99.99 W/m: 0.01 W/m , 100.0~999.9 W/m: 0.1 W/m ,1000~2000 W/m : 1 W/m 0.00~99.99 BTU/ft .h: 0.01 BTU/ ft .h, 100.0~634.0 BTU/ft .h: 0.1 BTU/ ft .h
		Angular Accuracy: Cosine Corrected < 7% (angle < 60°)
		Tilt Angle Range: 0~90°
		Tilt Angle Accuracy (at 23°C, 60% RH): ±1.2° (< 60°), Additional Temperature Induced Error±0.1°/°C from 23°C
		Sample Time: 0.4 sec.
		Operating Temp. & Relative Humidity: 0°C~50°C (32°F~122°F) Less than 80% RH
		Store Temp. & Relative Humidity: -10°C~60°C (14°F~140°F) Less than 85% RH
3.	Anemometer	Maximum length of telescopic vane: 890 mm
		Measuring range: 0.6 to 40 m/s
		Accuracy: ± (0.2 m/s + 1.5 % of mv)
		Resolution: 0.1 m/s

		Operation temperature: -20 to +50 °C
		Storage temperature: -40 to +70 °C
4.	Thermal hygrometer	Measuring Range: 0 to +50 °C -20 to +50 °C td
		Accuracy: ±1 digit: ±0.5 °C (at +25 °C)
		Resolution: 0.1 °C
		Operating temperature: 0 to +50 °C
		Measuring rate: 18 s
		Storage temperature: -40 to +70 °C
5.	Tachometer	Measuring Range: +1 to +99999 rpm
		Accuracy: ±1 digit: ±0.02% of m.v.
		Resolution: 0.01 rpm (+1 to +99.99 rpm) 0.1 rpm (+100 to +999.9 rpm) 1 rpm (+1000 to +99999 rpm)
		Operating temperature: 0 to +50 °C
		Storage temperature: -20 to +70 °C
6.	Multi meter	True RMS measurement

		Basic accuracy: 0.1%
		Voltage measuring range: 0.1 mV to 1,000 V AC/DC
		Current measuring range: 0.1 μA to 10 A AC/DC
		Resistance measuring range: 0.1 to 60 MΩ
		Frequency measuring range: 0.001 Hz to 30 MHz
		Capacitance measuring range: 0.001 nF to 30,000 μF
		Operating Temperature: -10 to +50 °C
		Storage temperature: -15 to +60 °C
7.	Thermocouple cable	K- type Teflon cable
8.	Temperature Indicator	Input: K type
		Resolution: 0.1°C
		No of Channel: 12
		Channel Selection: Through Rotary Switch.
		Supply: 230VAC. ±10%, 50 / 60Hz

3.3. *Experimentation*

Experiments were performed with conventional cylindrical SCPP model on 10-12, September 2019 at the Department of Mechanical Engineering, Delhi Technological University (DTU) (Delhi), India (28.75^0 N latitude, 77.11^0 E longitude) during 08:00 hours to 18:00 hours. The readings were taken on hourly basis. The experimental model dimension was taken on the basis of space constraint and ease of manufacturing and is shown in Table 3.

3.4. *Numerical computation*

For the traditional cylindrical SCPP experimental model in natural convection environment, the following thermal performance indicators are determined.

3.4.1. *Convective heat transfer coefficient (natural convection mode)*

The Convective heat transfer coefficient is the indicator of heat loss from solar collector to air. The Convective heat transfer coefficient can be calculated as [36]–[38] :

$$h_{cv} = 0.884 \times \left[\left(T_{gd} - T_{ch,in}\right) + \frac{\left[\left(P(T_{gd}) - Rh_{amb}\, P(T_{ch,in})\right)\right](T_{ch,in}+273)}{268900 - P(T_{gd})} \right]^{(1/3)} \quad (1)$$

3.4.2. *Coefficient of diffusivity*

The removal rate of moisture is a significant variable that is accountable for drying in natural convection mode within the solar collector greenhouse dryer. The greater speed of removal of moisture decreases the time of drying.

Instantaneous thermal loss efficiency factor for the canopy is an indirect loss for passive dryer and it can be evaluated as [32], [39], [40] :

$$\eta\, ith, canopy = \frac{U \sum A_i \left(T_{ch,in} - T_{amb}\right)}{I_g\, A_{tray}} \quad (2)$$

The experiment is performed in a no-load state for natural convection. Therefore, the sum of the efficiency factor of instantaneous thermal loss by canopy and ventilation is considered as unity [40], [41] :

$$\eta\, ith, vent \;=\; 1 \;-\; \eta\, ith, canopy \tag{3}$$

By using equations (2) and (3), coefficient of diffusivity can be defined as [39]–[41] :

$$C_{df} = \frac{\left(1-\eta_{ith,canopy}\right) I_g\, A_{tray}}{\left[n\, A_{chimney} \left[\frac{2\Delta P}{\rho}\right]^{1/2} \times \Delta P\right]} \tag{4}$$

3.4.3 *Heat loss factor*

Due to reduced density, the excess air absorption within the greenhouse dryer is accountable for shifting warm air into the ventilator. This type of heat loss factor can be articulated as [41]–[43]:

$$Q_{lf} = \; C_{df} \times A_{chimney} \times \left(\frac{2\Delta P}{\rho}\right)^{1/2} \times \Delta P \tag{5}$$

3.4.4. *Heat Utilization Factor (HUF)*

Heat utilization factor (HUF) is a temperature reduction ratio due to air cooling and temperature and temperature increase due to heating of air [44] :

$$HUF = \frac{\left(T_{gd} - T_{ch,in}\right)}{\left(T_{gd} - T_{amb}\right)} \tag{6}$$

3.4.5. *Coefficient of Performance (COP)*

Coefficient of performance (COP) is the ratio of difference of temperature between chimney inlet and surrounding & ground and surrounding [44]:

$$COP = \frac{\left(T_{ch,in} - T_{amb}\right)}{\left(T_{gd} - T_{amb}\right)} \tag{7}$$

3.5. *Exergy Analysis*

The exergy of the system is evaluated based on first law of energy balance equation. Assuming steady flow, the exergy equation can be written as [45] :

$$E_x = m_{amb.} C_{p,dry\ amb} \left[(T - T_{amb}) - T_{amb}\ ln \left[\frac{T}{T_{amb}} \right] \right] \quad (8)$$

The exergy equation, from where the air is entering, can be written as [45] :

$$E_{x\ inlet} = m_{amb}\ C_{p,dry\ amb} \left[\left(T_{ch,in} - T_{amb} \right) - T_{amb}\ ln \left[\frac{T_{ch,in}}{T_{amb}} \right] \right] \quad (9)$$

The exergy equation, from where the air is going out, can be written as:

$$E_{x\ outlet} = m_{amb}\ C_{p,dry\ amb} \left[\left(T_{ch,out} - T_{amb} \right) - T_{amb}\ ln \left[\frac{T_{ch,out}}{T_{amb}} \right] \right] \quad (10)$$

Exergy losses for drying under passive mode can be composed as [45] :

$$E_{x\ loss} = E_{x\ inlet} - E_{x\ outlet} \quad (11)$$

Exergy efficiency is defined as "The ratio of the exergy use to dry out the crop or product to the exergy of air supplied to the system for drying the product" [31]

Therefore the exergy efficiency of the system can be written as [45] :

$$\eta_{Ex} = \frac{E_{x\ outlet}}{E_{x\ inlet}} = 1 - \frac{E_{x\ loss}}{E_{x\ inlet}} \quad (12)$$

3.6 *EXPERIMENTAL UNCERTAINITY ANALYSIS*

Every measuring instrument consists of an uncertainty which can be evaluated by the measurement's precision. Measurement should be performed with care to minimize the likelihood of mistake. For surrounding temperature and ground temperature, which were the delicate parameter, the experimental uncertainty was calculated. Experimental uncertainty proportion is equal to the sum of internal & external uncertainty proportion. Least count of any measuring equipment is the external uncertainty, while internal proportion of uncertainty is determined as:

$$\%\ internal\ uncertainty\ U' = \left(\frac{U'}{mean\ of\ total\ observation} \times 100 \right) \quad (13)$$

Internal uncertainty, U' can be evaluated as:

$$U' = \frac{\sqrt{\sigma_1^2+\sigma_2^2+\sigma_3^2+\cdots\sigma_n^2}}{N} \quad (14)$$

Standard deviation is expressed as:

$$\sigma' = \frac{\sqrt{\sum(X_i-\bar{X})^2}}{N_0'} \quad (15)$$

Where$(X_i - \bar{X})$ is the mean deviation, N & N_0' are the no. of sets and no of observation in each set respectively. Experimental uncertainty (%) for canopy air temperature and inside canopy ground temperature observed inside the canopy is given in Table 5.

Table 5: Experiment percentage uncertainty for system temperature measurement.

S.No.	Parameters	Experimental uncertainty (%)		
		Internal	External	Total
1.	Ambient temperature	0.28	0.1	0.38
2.	Ground temperature	0.30	0.1	0.40

CHAPTER-4

RESULTS AND DISCUSSIONS

This chapter deals with the results obtained from performing the experiment on conventional cylindrical SCPP model and also discusses the obtained results. The experiment for three days are compared. Day 1 & 2 was clear sky condition while day 3 was cloudy condition. The performance parameters are calculated and compared for three days under different condition. Furthermore, the convective heat transfer coefficient, COP, HUF, C_{df}, Q_{lf}, exergy efficiency are also analyzed and discussed about. Also, the performance characteristic curve and equations are developed.

4.1 *Effect of different system temperatures w.r.t global and diffused solar radiation with time of the day.*

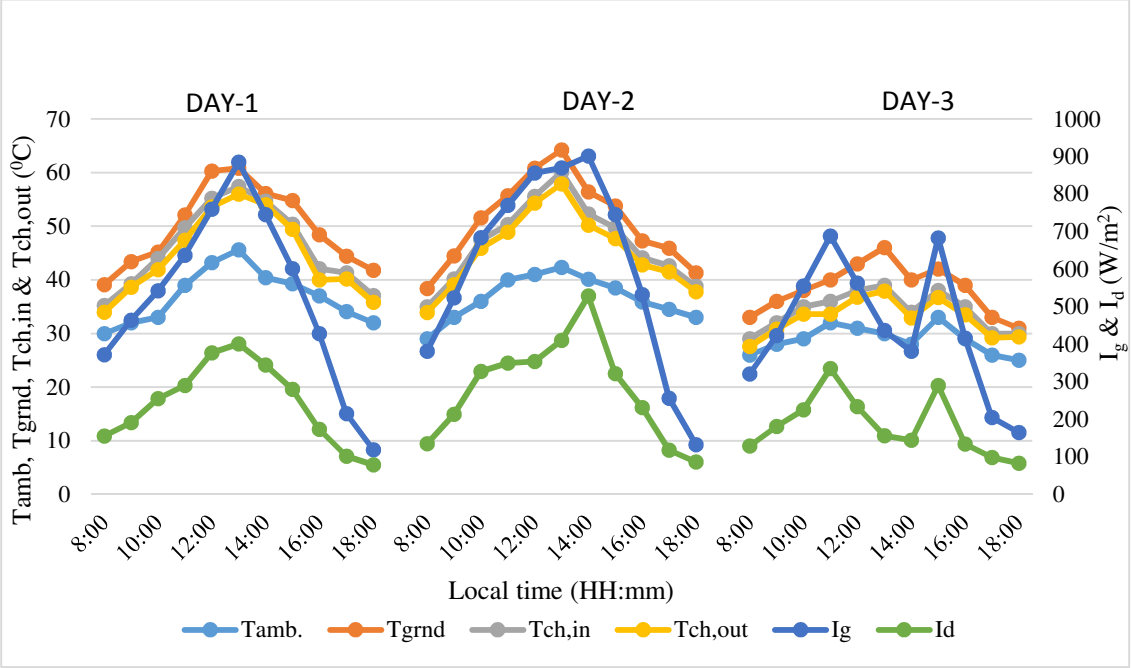

Fig 4.1: Variation of canopy ground temperature, chimney inlet temperature & chimney outlet temperature w.r.t solar radiation and ambient temperature with local time of the day.

Inside canopy temperature & surrounding temperature and global solar radiation are directly proportional to each other. Fig 4.1 shows the Variation of greenhouse ground

temperature, chimney inlet temperature & chimney outlet temperature w.r.t surrounding air temperature and global solar radiation with local time of the day. As the global solar radiation increases, its effect can be seen on various temperature as ground and ambient temperature also starts increasing. Highest global solar radiation on day 1, 2 and 3 was found to be 885 W/m^2, 901 W/m^2 and 688 W/m^2 respectively. Ground temperature was always found to be the highest w.r.t to ambient temperature. The maximum ground temperature was 60.8^{0}C, 64.2^{0}C and 46^{0}C for day 1, 2 and 3 respectively and highest ambient temperature was 45.6^{0}C, 42.3^{0}C and 32^{0}C for day 1, 2 and 3 respectively. The peak temperatures are recorded at 13:00 hours on day 1, 2 and 3. On day 1, 2 there is clear condition while at day 3 there is hazy and cloudy condition.

4.2 *Effect of velocity and relative humidity w.r.t time of the day.*

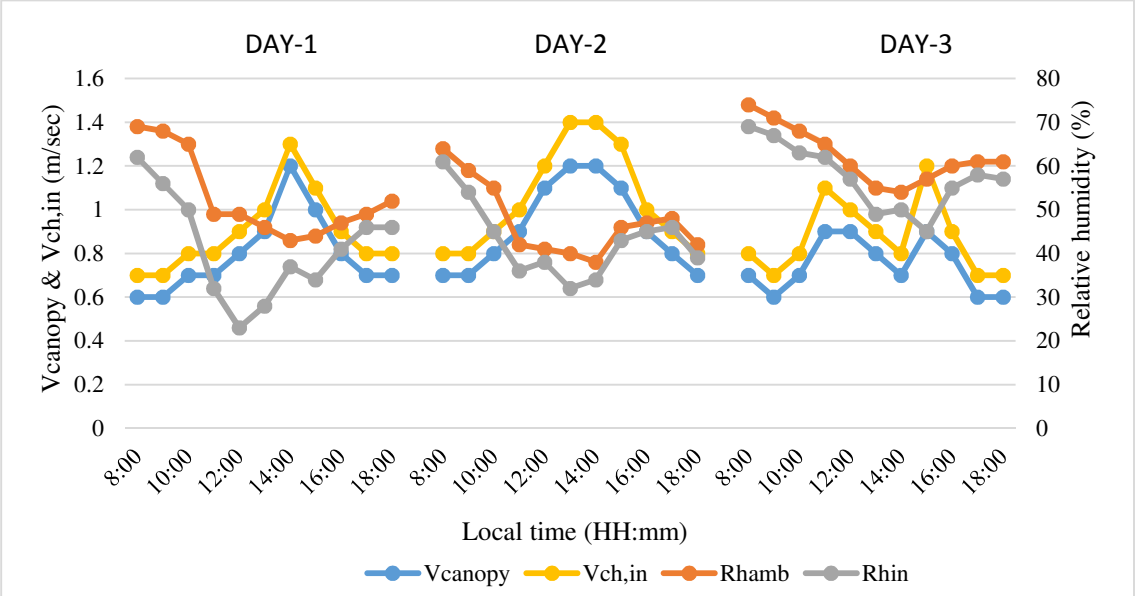

Fig 4.2: Variation of canopy velocity, chimney inlet velocity and greenhouse relative humidity w.r.t ambient temperature with time of the day.

The same amount of water vapor results in higher relative humidity in cool air than in warm air. As the air enters the greenhouse, due to increase in temperature there is increase in velocity of air inside greenhouse w.r.t to ambient air velocity because the density of air decreases and air tends to move towards the narrow chimney inlet along the height of the chimney. The increase in temperature inside the canopy increases the rate of moisture

removal and hence the relative humidity inside the greenhouse decreases. The velocity of air at chimney inlet was found to be higher than the velocity of air at entry of canopy. Fig 4.2 shows that the maximum canopy velocity and chimney inlet velocity was 1.2 m/sec, 1.2 m/s, 0.9 m/s & 1.3 m/s, 1.4 m/s, 1.1 m/s at day 1, 2 and 3 respectively. The maximum surrounding air relative humidity and inside canopy air relative humidity recorded was 69%, 64%, 74% and 62%, 61%, 69% at day 1, 2 and 3 respectively.

4.3 *Effect of convective heat transfer coefficient under natural convection with time of the day.*

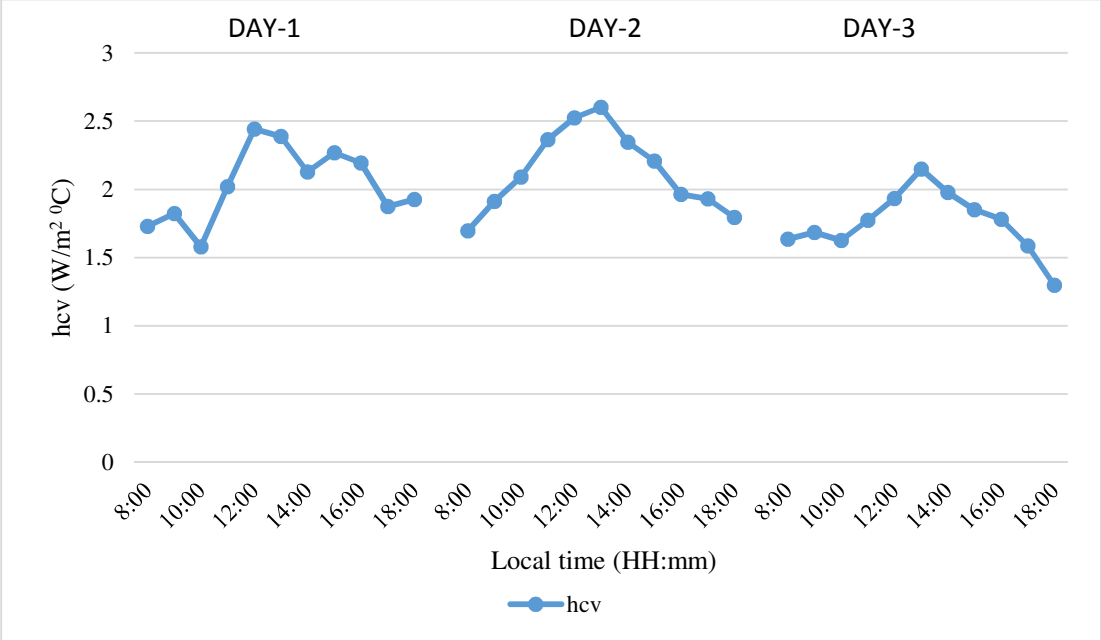

Fig 4.3: Variation of convective heat transfer coefficient with time of the day.

Variation of h_{cv} is shown in Fig. 4.3. The maximum value of h_{cv} on day 1 at 12:00 hours was 2.44 W/m^2 ^{0}C, on day 2 at 13:00 hours was 2.60 W/m^2 ^{0}C, on day 3 at 13:00 hours was 2.14 W/m^2 ^{0}C. The overall maximum value of h_{cv} was recorded on day 2 at 13:00 hours. The average value of h_{cv} on day 1 was 2.03 W/m^2 ^{0}C, on day 2 was 2.13 W/m^2 ^{0}C, on day 3 was 1.75 W/m^2 ^{0}C. The value of convective heat transfer coefficient decreases on day 3 due to cloudy weather. The average, maximum, minimum values of h_{cv} is given in Table 6. The higher value of h_{cv} suggests that there is high rate of conversion from solar radiation to heat energy.

Table 6: Average, maximum and minimum value of convective heat transfer coefficient.

S.no.	Day	Minimum value of hcv ($W/m^2\ ^0C$)	Maximum value of hcv ($W/m^2\ ^0C$)	Average value of hcv ($W/m^2\ ^0C$)
1.	Day 1	1.57	2.44	2.03
2.	Day 2	1.69	2.60	2.13
3.	Day 3	1.29	2.14	1.75

4.4 *Effect of HUF and COP with time of the day.*

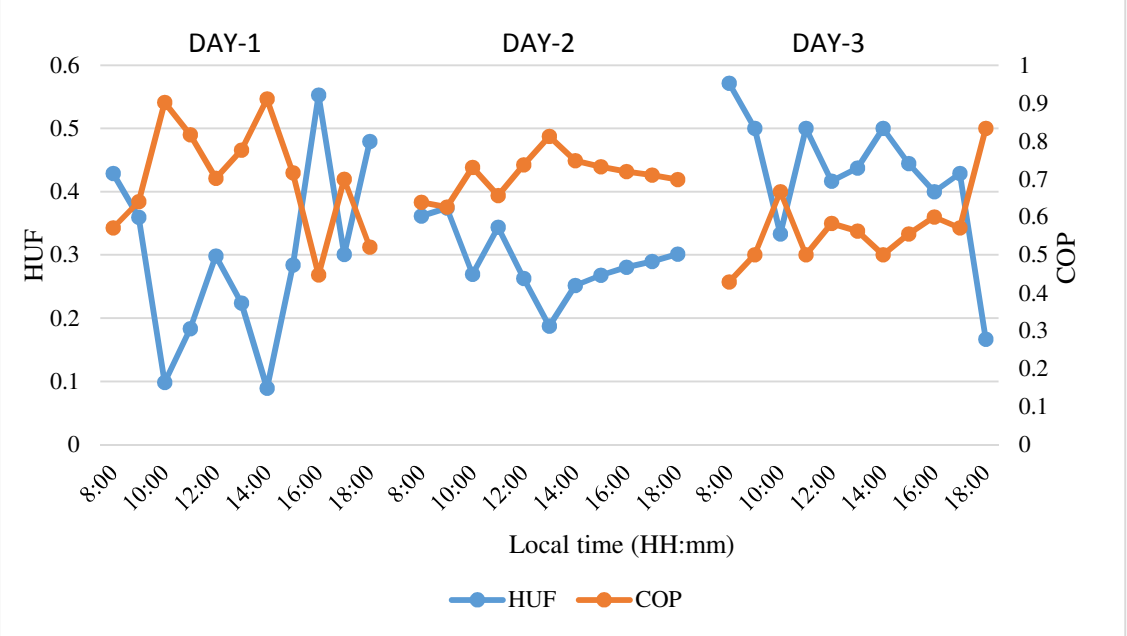

Fig. 4.4: Variation of HUF and COP with time of the day.

Fig. 4.4 shows the changes of HUF and COP with time. Variation of HUF during day 1 experimentation was 0.08-0.55, during day 2 was 0.18-0.37 and during day 3 was 0.16-0.57.

COP varies from 0.44-0.91 during day 1, 0.62-0.81 during day 2 and 0.42-0.83 during day 3. The highest value of HUF observed day 3 of experimentation was 0.57. The maximum value of COP was 0.91 during day 1 of experiment.

4.5 *Effect of Qlf with time of the day.*

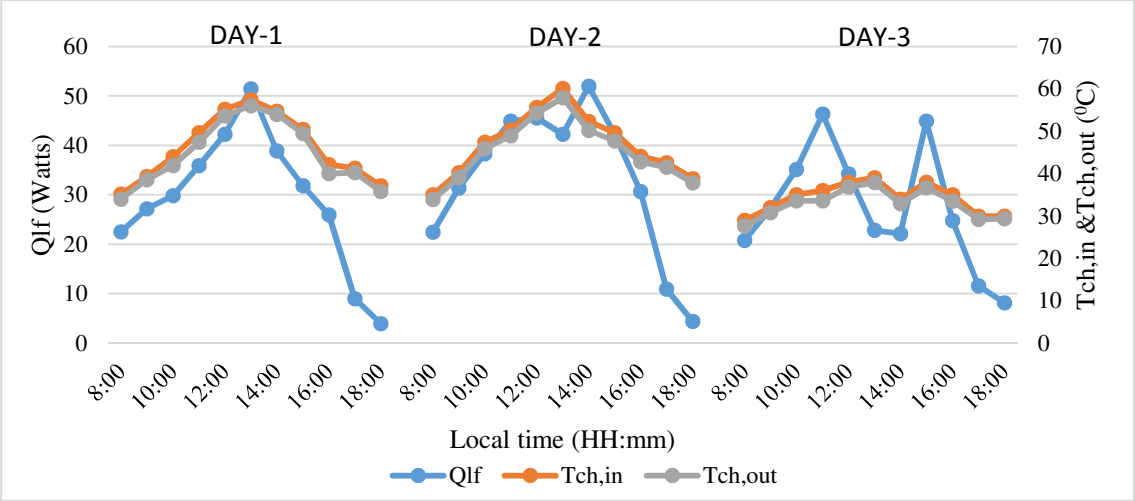

Fig. 4.5: Variation of heat loss factor w.r.t chimney inlet temperature, chimney outlet with time of the day.

With the help of C_{df}, heat loss factor through chimney variation is calculated by using equation (5) and its variation with chimney inlet and outlet temperature w.r.t time is shown in Fig. 4.5. As the temperature at inlet and outlet of chimney increases, heat losses by convection and conduction also increases along the length of chimney. The maximum value of Qlf was 51.42 watts, 51.93 watts, 46.29 watts during day 1, 2 and 3 of experimentation respectively. The average value of Qlf was 28.95 watts, 33.17 watts and 27.10 watts during day 1, 2 and 3 respectively.

Due to clouds condition, the sudden differences are observed on the day 3 of experiment. I_g & I_d values are also influenced by clouds and it deviates rapidly. Global solar radiation is considered as a significant parameter for heat energy production and heat loss factor. Wind velocity is another key factor to be considered for heat loss factor. As the wind velocities are higher, the Qlf also tends to be higher. As the fluctuation of wind velocity on day 3 was very high, the variation in Qlf was also very rapid. The maximum, minimum and average values of heat losses is given below in Table 7.

Table 7: Average, maximum and minimum value of heat loss factor.

S.no.	Day	Maximum value of Qlf (watts)	Minimum value of Qlf (watts)	Average value of Qlf (watts)
1.	Day 1	51.42	3.93	28.96
2.	Day 2	51.93	4.38	33.17
3.	Day 3	46.29	8.18	27.10

4.6 *Effect of exergetic efficiency and exergy loss with time of the day.*

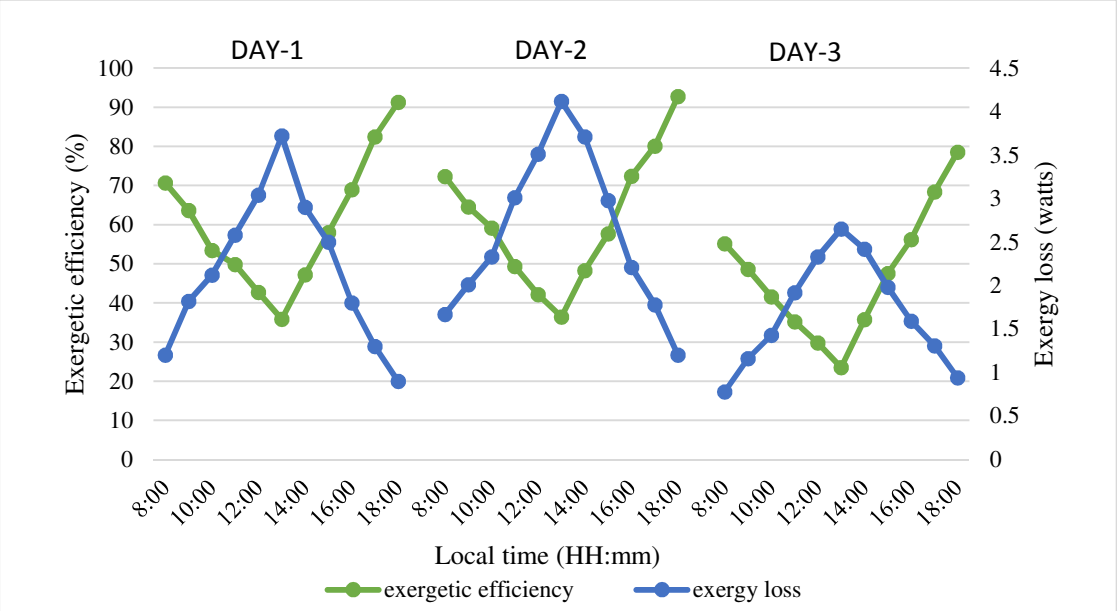

Fig. 4.6: Variation of exergetic efficiency and exergy loss with time of the day.

Fig. 4.6 shows the variation of exergetic efficiency and exergy loss with time of the day. Exergy analysis during drying process via natural solar dryer process under passive mode was obtained by using the results obtained from the experimentation of 3 days. In the drying experiment, the exergy losses increases from 8:00 hours to 13:00 hours and then there is a significant fall of exergy losses from 13:00 hours to 18:00 hours. As the solar radiation increases, exergy losses also tends to increase as convective heat transfer coefficient increases and vice versa. Exergetic efficiency follows the opposite trend of exergy loss. By using equation (12), it can be verified that if exergy losses increases, the exergetic efficiency will decrease. Therefore, exergetic efficiency is minimum where

exergy losses are maximum and vice versa. The exergetic efficiency varies from 35.82% to 91.26% during day 1, 36.43% to 92.74% during day 2 and 23.49% to 78.52% during day 3.The average, maximum and minimum values of exergetic efficiency is given in Table 8.

The variation of exergy losses during day 1 was 0.92 watts to 3.72 watts, during day 2 was 1.2 watts to 4.12 watts and during day 3 was 0.78 watts to 2.65 watts. The average, maximum and minimum values of exergy losses is given in Table 9.

Table 8: Average, maximum and minimum exergetic efficiency.

S.no.	Day	Average exergetic efficiency (%)	Maximum exergetic efficiency (%)	Minimum exergetic efficiency (%)
1.	Day 1	60.35	91.26	35.82
2.	Day 2	61.36	92.74	36.43
3.	Day 3	47.29	78.52	23.49

Table 9: Average, maximum and minimum exergy losses.

S.no.	Day	Average exergy losses (watts)	Maximum exergy losses (watts)	Minimum exergy losses (watts)
1.	Day 1	2.17	3.72	0.9
2.	Day 2	2.59	4.12	1.2
3.	Day 3	1.68	2.65	0.78

4.7 *Effect of coefficient of diffusivity with time of the day.*

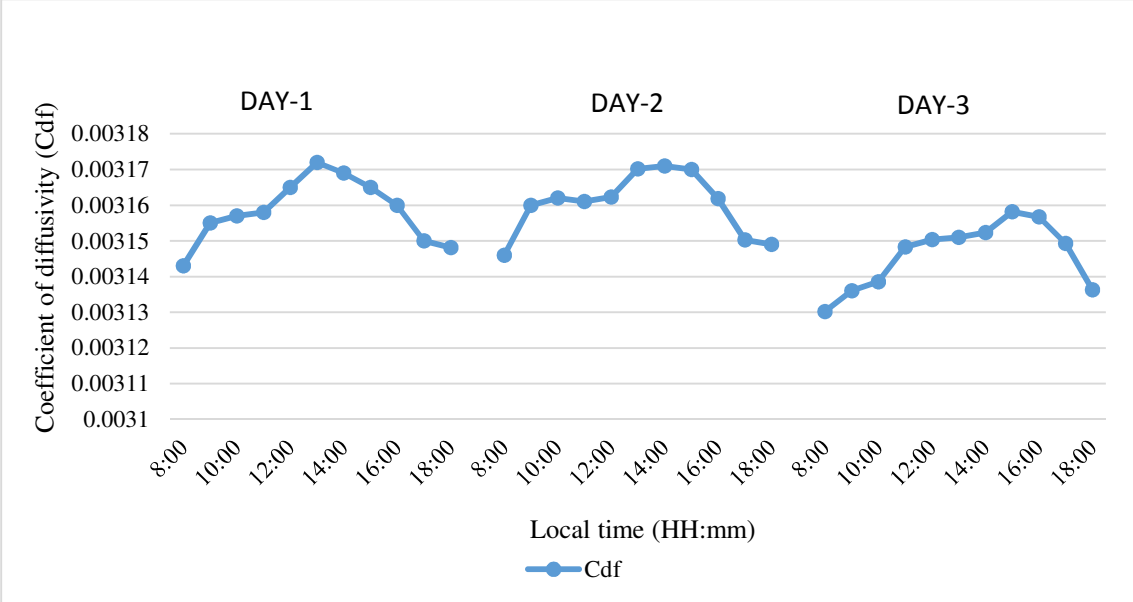

Fig. 4.7: Variation of coefficient of diffusivity with time of the day.

Fig. 4.7 depicts the variation of C_{df} with time. C_{df} can be calculated by using equation (4). The C_{df} is a very sensitive parameter. The significant parameters on which C_{df} depends on are solar radiation, inside greenhouse temperature of air and ambient temperature. Generally C_{df} has peak value during afternoon and lesser value during morning and evening time of the day. The variation of C_{df} on day 1 was from 0.003143 to 0.003172, on day 2 was 0.003146 to 0.003171 and on day 3 from 0.003130 to 0.003136.

Higher value of C_{df} depicts that there is high probability of heat loss through the height of the chimney while lower value shows the incapability of fresh and cold ambient air to replace hot and humid greenhouse air which slows down the removal rate of moisture.

4.8 *DEVELOPMENT OF PERFORMANCE CHARACTERISTIC CURVE AND EQUATION IN NO-LOAD UNDER NATURAL CONVECTION MODE.*

Day 1, 10 September 2019 (clear sky condition), was considered to draw the characteristic curve and its equation. The ambient temperature was varying from 30^0C to 45.6^0C and

inside greenhouse temperature was varying from 35.2^{0}C to 57.4^{0}C.The horizontal axis is ($T_{ch,\,in} - T_{amb}$)/I_g and the vertical axis is instantaneous indirect thermal loss efficiency ($\eta_{ith\ canopy}$). The characteristic curve generally comes out to be a straight line.

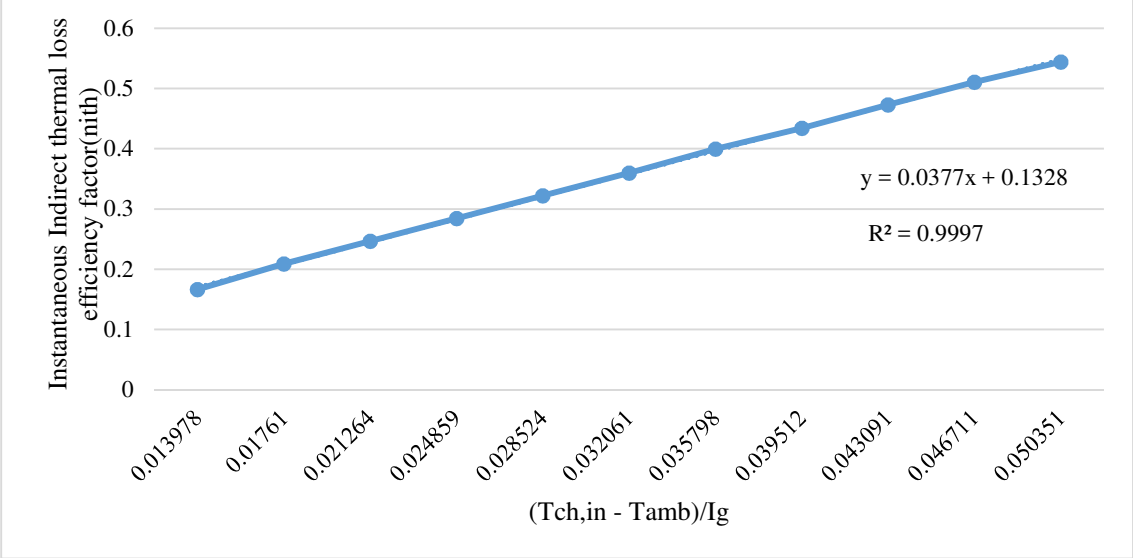

Fig. 4.8: Variation of instantaneous efficiency factor vs. $\frac{T_{ch,in}-T_{amb}}{I_g}$ in no-load for natural convection mode greenhouse dryer.

Fig. 4.8 shows the performance characteristic curve under no-load natural convection mode for greenhouse solar dryer.

Using the least square method, the characteristic curve equation for SCPP as follows

$$\eta_{ith,canopy} = 0.1328 + 0.0377\left(\frac{T_{ch,in}-T_{ch,out}}{I_g}\right) \quad (16)$$

The above obtained characteristic equation for SCPP greenhouse dryer under natural convection, the instantaneous indirect thermal loss efficiency factor is identical to the results obtained under natural convection for a modified greenhouse dryer.[46] and they have also verified their results experimentally with the results of flat plate collector [47].

CHAPTER-5

CONCLUSION

The conclusions drawn for the system of SCPP with solar dryer on the basis of experimental results are as follows:

1. For the SCPP with solar dryer, the maximum inside canopy ground temperature recorded was at 64.2^0C.
2. The experimental percentage uncertainty found to be 0.38 and 0.40 for ambient air and ground temperature measurement which was found within the permissible limit.
3. The maximum convective heat transfer coefficient (h_{cv}) was found on day 2 i.e. 2.60 W/m^2 ^{0}C which was 6.15% and 17.69% more than day 1 and 3 respectively.
4. The highest exergetic efficiency under passive mode was 91.26%, 92.74% and 78.52% during day 1, 2 and 3 of experimentation respectively.
5. The maximum heat loss factor was 51.42 watts, 51.93 watts and 46.29 watts on day 1, 2 and 3 experimentation respectively
6. The maximum heat utilization factor was found 0.55, 0.37 and 0.57on day 1, 2, 3 experimentation respectively.
7. The maximum COP was found 0.91, 0.81 and 0.83 on day 1, 2, and 3 experimentation respectively.
8. Experimental results and estimated thermal performance parameters of SCPP validate the effectiveness of the system.
9. The maximum coefficient of diffusivity was 0.003172, 0.003171 and 0.003136 during day 1, 2 and 3 of experimentation.
10. The characteristic equations developed was validated through experimental results of John A. Duffie [47]. When these parameters are known, the values of $x = (T_{ch,in} - T_{amb})/I_g$. Therefore, by using these characteristic formulas for solar dryer, a comparison of efficiencies can be created.
11. The highest temperature recorded was 64.2^0C, hence the system of solar dryer can be recommended for drying vegetables and grains like corn, maize, paddy, pulses, rice, wheat, brinjal, cabbage, garlic, onion, tomatoes.

REFERENCES

[1] S. Shafiee and E. Topal, “When will fossil fuel reserves be diminished?,” *Energy Policy*, vol. 37, no. 1, pp. 181–189, 2009.

[2] M. M. Halmann and M. Steinberg, *In Reply: BEHAVIOUR THERAPY*. USA, 1999.

[3] N. L. Panwar, S. C. Kaushik, and S. Kothari, “Role of renewable energy sources in environmental protection: A review,” *Renew. Sustain. Energy Rev.*, vol. 15, no. 3, pp. 1513–1524, 2011.

[4] N. Lewis, “Toward cost effective solar energy use,” *Science (80-.).*, vol. 315, no. 5813, pp. 798–801, 2007.

[5] A. J. Nozik, “Photoelectrochemistry:Application to solar energy conversion,” *Annu. Rev. Phys. Chem.*, vol. 29(1), pp. 189–222, 1978.

[6] G. Jungmeier and G. Marlandii, “TOWARDS A STANDARD METHODOLOGY FOR GREENHOUSE GAS BALANCES OF BIOENERGY SYSTEMS IN COMPARISON WITH FOSSIL ENERGY SYSTEMS B.,” *Biomass and Bioenergy*, vol. 13, no. 6, pp. 359–375, 1997.

[7] International Energy Agency, “Global Energy & CO2 Status Report,” *Glob. Energy CO2 Status Rep.*, no. March, pp. 1–15, 2018.

[8] International Energy Agency, “Global engagement,” 2017. [Online]. Available: https://www.iea.org/countries/India/.

[9] “Electricity sector in India,” 2019. [Online]. Available: https://en.wikipedia.org/wiki/Electricity_sector_in_India.

[10] Government of India, “All India Installed Capacity (in Mw) of Power Stations Installed Capacity (in Mw) of Power Utilities in the States / Uts Located in,” *Cent. Eectricity Authority, Minist. power*, vol. 4, pp. 1–7, 2018.

[11] “Power sector at a glance ALL INDIA,” 2019. [Online]. Available: https://powermin.nic.in/en/content/power-sector-glance-all-india.

[12] "MNRE Report 2017-18," 2018.

[13] A. Dhahri and A. Omri, "A Review of solar Chimney Power Generation Technology," *IJEAT*, vol. 2, no. 3, pp. 1–17, 2013.

[14] S. F. Jones, *Engineering strategies for greenhouse gas mitigation*. New York: Cambridge University Press, 2011.

[15] M. Mehrpooya, M. Shahsavan, and M. M. M. Sharifzadeh, "Modeling, energy and exergy analysis of solar chimney power plant-Tehran climate data case study," *Energy*, vol. 115, pp. 257–273, 2016.

[16] T. W. Von Backström *et al.*, "State and recent advances in research and design of solar chimney power plant technology," *VGB PowerTech*, vol. 88, no. 7, pp. 64–71, 2008.

[17] A. Demirbas, "Biofuels securing the planet's future energy needs," *Energy Convers. Manag.*, vol. 50, no. 9, pp. 2239–2249, 2009.

[18] J. Schlaich, "The Solar Chimney: Electricity fron the sun," *J. Power Energy Eng.*, vol. 4, 1995.

[19] F. Denantes and E. Bilgen, "Counter rotating turbines for solar chimney power plants," *Renew. energy*, vol. 31, no. 12, pp. 1873–1891, 2006.

[20] S. Hu, D. Y. C. Leung, and M. Z. Q. Chen, "Effect of Divergent Chimneys on the Performance of a Solar Chimney Power Plant," *Energy Procedia*, vol. 105, pp. 7–13, 2017.

[21] M. A. H. Abdelmohimen and S. A. Algarni, "Numerical investigation of solar chimney power plants performance for Saudi Arabia weather conditions," *Sustain. Cities Soc.*, vol. 38, no. December 2017, pp. 1–8, 2018.

[22] Y. Xu and X. Zhou, "Performance of divergent-chimney solar power plants," *Sol. Energy*, vol. 170, no. May, pp. 379–387, 2018.

[23] O. A. Najm and S. Shaaban, "Numerical investigation and optimization of the solar chimney collector performance and power density," *Energy Convers.*

Manag., vol. 168, no. April, pp. 150–161, 2018.

[24] N. Fadaei, A. Kasaeian, A. Akbarzadeh, and S. H. Hashemabadi, "Experimental investigation of solar chimney with phase change material (PCM)," *Renew. Energy*, vol. 123, pp. 26–35, 2018.

[25] N. Fathi *et al.*, "Efficiency enhancement of solar chimney power plant by use of waste heat from nuclear power plant," *J. Clean. Prod.*, vol. 180, pp. 407–416, 2018.

[26] N. Jafarifar, M. M. Behzadi, and M. Yaghini, "The effect of strong ambient winds on the efficiency of solar updraft power towers: A numerical case study for Orkney," *Renew. Energy*, pp. 937–944, 2019.

[27] Y. Amudam and V. P. Chandramohan, "Influence of thermal energy storage system on flow and performance parameters of solar updraft tower power plant: A three dimensional numerical analysis," *J. Clean. Prod.*, vol. 207, pp. 136–152, 2019.

[28] A. Hassan, M. Ali, and A. Waqas, "Numerical investigation on performance of solar chimney power plant by varying collector slope and chimney diverging angle," *Energy*, vol. 142, pp. 411–425, 2018.

[29] R. Balijepalli, V. P. Chandramohan, and K. Kirankumar, "Performance parameter evaluation, materials selection, solar radiation with energy losses, energy storage and turbine design procedure for a pilot scale solar updraft tower," *Energy Convers. Manag.*, vol. 150, no. July, pp. 451–462, 2017.

[30] P. J. Cottam, P. Duffour, P. Lindstrand, and P. Fromme, "Effect of canopy profile on solar thermal chimney performance," *Sol. Energy*, vol. 129, pp. 286–296, 2016.

[31] A. Akbulut, A., Durmus, "Energy and exergy analysis of thin layer drying of mulberry in a forced solar dryer," *Energy*, vol. 35, pp. 1754–1763, 2010.

[32] O. Prakash and A. Kumar, "Performance evaluation of greenhouse dryer with opaque north wall," *Heat Mass Transf. und Stoffuebertragung*, vol. 50, no. 4, pp.

493–500, 2014.

[33] R. Dev and G. N. Tiwari, “Characteristic equation of a passive solar still,” *Desalination*, vol. 245, no. 1–3, pp. 246–265, 2009.

[34] O. Prakash, A. Kumar, and V. Laguri, “Performance of modified greenhouse dryer with thermal energy storage,” *Energy Reports*, vol. 2, pp. 155–162, 2016.

[35] P. S. Chauhan and A. Kumar, “Heat transfer analysis of north wall insulated greenhouse dryer under natural convection mode,” *Energy*, vol. 118, pp. 1264–1274, 2017.

[36] A. Kumar and G. N. Tiwari, “Thermal modeling of a natural convection greenhouse drying system for jaggery: An experimental validation,” *Sol. Energy*, vol. 80, no. 9, pp. 1135–1144, 2006.

[37] S. Singh and S. Kumar, “Development of convective heat transfer correlations for common designs of solar dryer,” *Energy Convers. Manag.*, vol. 64, pp. 403–414, 2012.

[38] D. Jain, “Determination of Convective Heat and Mass Transfer Coefficients for Solar Drying of Fish,” *Biosyst. Eng.*, vol. 94, no. 3, pp. 429–435, 2006.

[39] O. Prakash and A. Kumar, “Annual performance of a modified greenhouse dryer under passive mode in no-load conditions,” *Int. J. Green Energy*, vol. 12, no. 11, pp. 1091–1099, 2015.

[40] O. Prakash and A. Kumar, “Development and testing of modified greenhouse dryer under natural convection,” *Heat Transf. Res*, vol. 45, pp. 431–51, 2014.

[41] P. Barnwal and A. Tiwari, “Design, construction,testing of hybrid photovoltaic integrated greenhouse dryer,” *Int J Agric Res*, vol. 3(2), pp. 110–20, 2008.

[42] G. N. Tiwari, “Greenhouse technology for controlled environment,” pp. 184–5, 2003.

[43] R. Gupta, G. N. Tiwari, and A. Gupta, “Calculation of total solar fraction for different orientation of greenhouse using 3D shadow analysis in auto CAD,”

Energy build, vol. 47, no. 27–34, 2012.

[44] G. N. Tiwari, "Fundamental of solar dryers," *Anamaya Publ.*, pp. 263–4, 2009.

[45] Fudholi, A., Ruslan, M.H., Othman, M.Y., Azmi, M.S.M., Zaharim, A., Sopian, K., "Drying of palm oil fronds in solar dryer with finned double pass solar collectors," *WSEAS Trans, Heat mass Transf.*, vol. 4(7), pp. 105–114, 2013.

[46] O. Prakash and A. Kumar, "Design, development, and testing of a modified greenhouse dryer under conditions of natural convection," *Heat Transf. Res.*, vol. 45, no. 5, pp. 433–451, 2014.

[47] W. A. B. John A. Duffie, *Wiley: Solar Engineering of Thermal Processes, 4th Edition - John A. Duffie, William A. Beckman*. 2013.

[48] F. J and C. N, "Multi-stage, indirectly heated solar still," *Sol. energy*, vol. 44, pp. 215–223, 1990.

APPENDIX 1

Table 1(a): Expressions for saturated vapor pressure as function of temperature (^{0}C)

S. No.	P (N/m^2)	Range of T (℃)	Reference
1.	$exp\left[25.317 - \frac{5144}{(T+273.15)}\right]$	10-90	[48]

APPENDIX 2

Table 2(a): Expression for Overall heat transfer coefficient

S. No.	U (W/m^2K)	References
1.	$\frac{1}{U} = \left(\frac{1}{h_1}\right) + \left(\frac{l_g}{K}\right) + \left(\frac{1}{h_2}\right)$	[36]

Where,

$h_1 = h_{cv} + h_r$

$h_r = \sigma\varepsilon\left(T_g + 273.15\right)^3$

$h_2 = 5.7 + 3.8\upsilon$

APPENDIX-3

Table 3(a): Difference of inside canopy air temperature and surrounding air temperature & canopy ground temperature and inside canopy air temperature w.r.t global solar radiation and local time of the day.

Time	I_g (W/m^2)	$T_{ch,in} - T_{amb}$ (^{0}C)	$T_{gd} - T_{ch,in}$ (^{0}C)
Day 1			
8:00	372	5.2	3.9
9:00	464	7.3	4.1
10:00	542	11	1.2
11:00	637	10.7	2.4
12:00	760	12	5.1
13:00	885	11.8	3.4
14:00	745	14.3	1.4
15:00	601	11.1	4.4
16:00	428	5.1	6.3
17:00	215	7.2	3.1
18:00	119	5.1	4.7
Day 2			
8:00	381	6	3.4
9:00	524	7.2	4.3
10:00	684	11.4	4.2
11:00	770	10.3	5.4
12:00	856	14.6	5.2
13:00	870	17.8	4.1
14:00	901	12.2	4.1
15:00	745	11.2	4.1
16:00	532	8.2	3.2
17:00	256	8.1	3.3
18:00	132	5.8	2.5
Day 3			
8:00	321	3	4
9:00	423	4	4
10:00	555	6	3
11:00	688	4	4
12:00	563	7	5
13:00	437	9	7
14:00	381	6	6
15:00	683	5	4
16:00	416	6	4
17:00	205	4	3
18:00	165	5	1